First year progress report: Complex systems approach to cascading failures

Consortium for Electric Reliability Technology Solutions

December 2001

Prepared by

Benjamin A. Carreras
Oak Ridge National Laboratory
Oak Ridge, TN USA

Ian Dobson
Power Systems Engineering Research Center
University of Wisconsin-Madison
Electrical and Computer Engineering Department
1415 Engineering Drive
Madison WI 53706 USA

James S. Thorp
Power Systems Engineering Research Center
Cornell University
School of Electrical and Computer Engineering
Ithaca NY 14850 USA

ACKNOWLEDGEMENTS

The work described in this report was coordinated by the Consortium for Electric Reliability Technology Solutions and was funded by the Assistant Secretary for Energy Efficiency and Renewable Energy, Office of Power Technologies, Transmission Reliability Program of the U.S. Department of Energy under contract 9908935 and Interagency Agreement DE-A1099EE35075 with the National Science Foundation.

Part of this research has been carried out at Oak Ridge National Laboratory, managed by UT-Battelle, LLC, for the U.S. Department of Energy under contract number DE-AC05-00OR22725. Ian Dobson gratefully acknowledges support in part from National Science Foundation grant ECS-0085711. Ian Dobson thanks H-D. Chiang and the School of ECE at Cornell University for their generous hospitality during a sabbatical leave.

CONTENTS

1 INTRODUCTION

This document is the first year report of a two-year CERTS (Consortium for Electric Reliability Technology Solutions) project studying large scale blackouts and cascading failures of electric power transmission systems. The project is inventing new methods, models and analysis tools from complex systems, self-organized criticality, probability, and power systems engineering so that the risks of large blackouts and cascading failures can be understood and mitigated from novel global and top-down perspectives. The work is performed by close collaboration between Oak Ridge National Laboratory and the Power Systems Engineering Research Center at the University of Wisconsin-Madison and Cornell University.

Section 2 explains topics providing background to the project and sections 3 and 4 summarize first year progress and second year plans for the project. The details of the technical achievements of the project in the first year are documented in Section 6.

2 PROJECT BACKGROUND

2.1 GENERAL MOTIVATION

The United States electrical energy supply infrastructure is experiencing rapid changes and will continue to be operated closer to a stressed condition in which there is substantial risk of cascading outages and blackouts. The rapid changes in this highly complex system present significant challenges for maintaining its operational stability and reliability.

Management of the electrical power network to avoid catastrophic blackouts should account for the global dynamics of series of these blackouts and interdependencies between blackouts. Analysis of historical NERC data shows power tails in the distribution of blackout sizes; that is, there are many more large blackouts than expected. Simulation results to date also show underlying nontrivial complex dynamics and interdependencies. These complex dynamics between blackouts are of great significance if one wants to operate the system to avoid blackouts. For example, in other complex systems showing self-organized criticality (SOC), well-intentioned policies to avoid small "blackouts" can inadvertently lead to an increased frequency of large "blackouts". Moreover, features of the protection system such as "hidden failures" play an important role in cascading failures leading to blackouts. This project is designed to establish models and tools for a new global approach to cascading failures in stressed power systems, which will be complementary to the valuable and traditional efforts to analyze cascading events on a more individual cause-and-effect basis.

This project will develop the basic tools needed to represent demand-driven complex dynamical systems for electrical power transmission systems. The project will investigate the nature of the SOC-like and other complex dynamics concepts in cascading failures so that the prospects for controlling these global dynamics to mitigate catastrophic failures can be assessed.

The first year of the project will concentrate on improving, implementing and understanding models capturing the complex dynamics of series of blackouts. The second year of the project will concentrate on improving the realism of the models and data, trying to reproduce qualitative features of historical NERC data on blackouts, and assessing the prospects for controlling the complex model dynamics to mitigate or avoid large blackouts.

2.2 SELF-ORGANIZED CRITICALITY

The United States is dependent on the smooth functioning of a complex system of infrastructures such as electrical power transmission systems. Global disruptions of these systems can obviously cause severe damage to our society. To minimize such disruptions, it is necessary to understand, predict and control the response of complex systems to outside perturbations.

Complex natural systems are often governed by self-organized criticality. The concept of self-organized criticality brings together ideas of self-organization of nonlinear dynamical systems with the often observed near critical behavior of many natural phenomena. These phenomena exhibit self-similarities over extended ranges of spatial and temporal scales. In those systems, scale lengths may be described by fractal geometry and time scales that lead to 1/f-like power spectra. Self-organized criticality gives an intimate connection between the scale invariance in space and time [Bak87].

Physics applications include modeling the motion of tectonics plates [Carlson94], spin glass systems, and turbulent transport [Newman96a,96b,96c, Carreras96]. Simple cellular automata models have been very useful in reproducing the complexity of those systems. That is the case of the sand pile model that presents the complex structure of multiple ranges in the frequency spectrum including the ubiquitous 1/f regime [Hwa92]. SOC has also been applied to biological, ecological [Bak93] and economic models [Lo91, Mantegna95].

A characteristic property of SOC systems is that they relax through what we call events. These events can happen over all scales of the system. Examples of these events are: earthquakes, for the motion of tectonic plates; fires, for a forest evolution [Drossel92]; extinction, in the coevolution of biological species; and avalanches, in the dynamics of sand piles. In a time-averaged sense, these systems are subcritical (that is, they lie in an average state that should not trigger any events) and the relaxation events happen intermittently. The time spent in a subcritical state relative to the time of the events varies from one system to another. For instance, the chance of finding a forest on fire is very low with the frequency of fires being on the order of one fire every few years and with many of these fires small and inconsequential. Very large fires happen over time periods of decades or even centuries. However, because of their consequences, these large but infrequent events are the important ones to control and minimize. One of the main goals of the research on these systems is to understand how and when global events may happen in order to predict them.

In our society, systems such as power transmission grids, communication networks, transportation systems and market distribution networks have complex interconnections, are strongly driven and they tend to operate close to the limit of their capabilities. Therefore, they probably evolve to a self-organized critical state. In this state, global disruptions are unavoidable and intrinsically difficult to predict.

A complex society like ours is vulnerable to these types of global disruptions. Without outside interference, they happen over long time scales and in an apparently random fashion. Every particular event can be and generally is investigated on its own, and the cause or causes for the event are identified. Naturally, there are always reasonable explanations for each isolated event. However, what those isolated explanations miss is the underlying dynamics of the complex system and the fact that similar events will happen again from different causes. Interestingly, published analysis (EPRI) of the Northwestern power outages of July and August 1996 discuss both the specific causes such as insufficient reactive support and excessive tree growth as well as global system causes such as "big picture", latent failure conditions and transmission networks operating near operational limits. It is these latter causes that global SOC type modeling addresses.

2.3 HIDDEN FAILURES IN PROTECTION SYSTEMS

Five recent major Western Systems Coordinating Council (WSCC) events involved incorrect operations in the generator protection equipment or the line protection relays. As shown by these WSCC events, the initial act may be a fault clearing device working properly to prevent real damage to the equipment. However, history also shows that after the initial correct course of action, a series of unnecessary protection operations only served to propagate the initial disturbance and damage the security of the whole power system. These "mis-operations" are noted as the hidden failures embedded in the protection schemes that reveal themselves when the power system deviates toward an abnormal state. The current protection system's multiple overlapping mechanisms incline heavily toward dependability and promote hidden failures. Although the redundancy and over-protection in this design prevents any hardware damage, these "sympathy" trips of lines and generators present a danger to global power system security.

Due to the rarity of these types of cascading outages, the compounded effects of a series of unlikely protection operations have not been thoroughly studied. Moreover, even with advanced simulation techniques such as importance sampling, these cascading outages are time consuming to simulate [Thorp98, Thorp01]. There is a clear need to develop new methods to simulate, analyze and understand cascading outages due to hidden failures so that effective measures can be taken to mitigate or avoid these blackouts [Chen01].

2.4 EVIDENCE OF COMPLEX SYSTEM BEHAVIOR IN NERC BLACKOUT DATA

This section summarizes analyses of NERC blackout data from [Carreras01a]. Electric power transmission networks are complex systems that undergo major cascading disturbances, or blackouts. Individually, these blackouts can be attributed to specific causes such as weather or equipment failure. However, an exclusive focus on these individual causes can overlook the global dynamics of a complex system in which repeated major disruptions from a wide variety of sources are a virtual certainty.

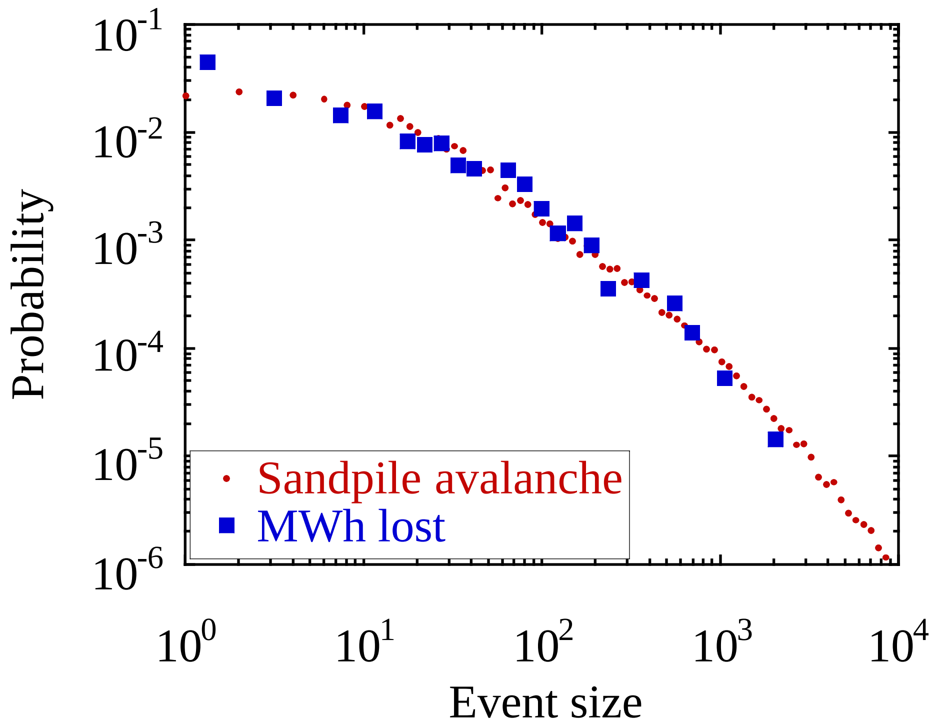

Figure 1. PDF of blackout sizes (MWh lost) compared to PDF of avalanche sizes from an SOC sandpile system.

We analyze a 15 year time series of blackout sizes obtained from NERC to probe the nature of these complex system dynamics. The blackout sizes are measured by the energy unserved (MWh). We plot the probability distribution function of the blackout sizes in Figure 1. The pdf has a power tail. Moreover, the same analysis applied to a time series of avalanche sizes from a sandpile model known to be self-organized critical gives results of the same form. Thus the blackout data is consistent with self-organized criticality. Self-organized criticality, if fully confirmed in power systems, would suggest new complex systems approaches to understanding and possibly controlling blackouts.

The strength of our conclusions is somewhat limited by the short time period (15 years) of the available blackout data. To further understand the mechanisms governing the dynamics of power system blackouts, modeling of the power system from a self-organized critical perspective is indicated and is further pursued in this project.

2.5 IDEAS OF SOC IN SERIES OF POWER SYSTEM BLACKOUTS

This section gives a qualitative account of the structure and effects in a large scale electric power transmission system which could give rise to SOC. This view of the power system complex dynamics underlies the OPA model that is described in detail in [Dobson01, Carreras01b]. This section is based on material from [Carreras00].

The transmission system contains many components such as generators, transmission lines, transformers and substations. Each component experiences a certain loading each day and when all the components are considered together they experience some pattern or vector of loadings. The pattern of component loadings is determined by the power system operating policy and is driven by the aggregated customer demands at the substations. The power system operating policy includes short time frame actions such as generator dispatch as well as longer time frame actions such as improvements in procedures and planned outages for maintenance. The operating policy seeks to satisfy the customer demands at least cost. The customer demand has daily and seasonal cycles and a secular increase. Moreover, the patterns of customer demand change due to the evolution of bulk power markets and geographic shifts in population and industry.

Events are either the limiting of a component loading to a maximum or the zeroing of the component loading if that component trips or fails. Events occur with a probability that depends on the component loading. For example, the probability of transformer failure generally increases with loading. Another example is that an operator redispatching to limit power flow on a transmission line to its thermal rating could be modeled as probability zero below the thermal rating of the line and probability one above the thermal rating.

Each event is a limiting or zeroing of load in a component and causes a redistribution of power flow in the network and hence a discrete increase in the loading of other system components. Thus events can cascade. If a cascade of events includes limiting or zeroing the load at substations, it is a blackout. A stressed power transmission system experiencing an event must either redistribute load satisfactorily or shed some load at substations in a blackout. A cascade of events leading to blackout usually occurs on a time scale of minutes to hours and is completed in less than one day.

It is customary for utility engineers to make prodigious efforts to avoid blackouts and especially to avoid repeated blackouts with similar causes. These responses to a blackout occur on a range of time scales longer than one day. Responses include repair of damaged equipment, more frequent maintenance, changes in operating policy away from the specific conditions causing the blackout, installing new equipment to increase system capacity, and adjusting or adding system alarms or controls. The responses reduce the probability of events in components related to the blackout, either by lowering their probabilities directly or by reducing component loading by increasing component capacity or by transferring some of the loading to other components. The responses are directed towards the components involved in causing the blackout. Thus the probability of a similar blackout occurring is reduced, at least until load growth degrades the improvements made. There are similar, but less intense responses to unrealized threats to system security such as near misses and simulated blackouts.

The pattern or vector of component loadings may be thought of as a system state. Maximum component loadings are driven up by customer demand trends via the operating policy. High loadings increase the chances of cascading events and blackouts. The loadings of components involved in the blackout are reduced or relaxed by the responses to security threats and blackouts. However, the loadings of some components not involved in the blackout may increase. These opposing forces driving the component loadings up and relaxing the component loadings are a reflection of the standard tradeoff between satisfying customer demands economically and security. The opposing forces apply over a range of time scales. We suggest that the opposing forces, together with underlying growth in customer demand and diversity give rise to a dynamic equilibrium and conjecture that this dynamic equilibrium is SOC.

We briefly indicate the roughly analogous structure and effects in an idealized sand pile model that is expected to show SOC [Bak96]. Consider a large, idealized sand pile that has grains of sand added at a continuously varying location. When the local maximum gradient gets too large, sand at that location is more likely to topple. Events are the toppling of sand and cascading events are avalanches. The system state is a vector of maximum gradients at all the locations in the sand pile. The driving force is the addition of sand, which tends to increase the maximum gradient, and the relaxing force is gravity, which topples the sand and reduces the maximum gradient. SOC is a dynamic equilibrium in which avalanches of all sizes occur and in which there are long time correlations between avalanches. The analogy between the sand pile and the power system is shown in Table 1. There are also some distinctions between the two systems. In the sand pile, the avalanches are coincident with the relaxation of high gradients. In the power system, each blackout occurs on fast time scale (less than one day), but the knowledge of which components caused the blackout determines which component loadings are relaxed both immediately after the blackout and for some time after the blackout.

Table 1. Analogy between power system and sand pile

	Power system	Sand pile
system state	loading pattern	gradient profile
driving force	customer demand	addition of sand
relaxing force	response to blackout	gravity
event	limit flow or trip	sand topples

To summarize, we have given a qualitative description of the global dynamics of a large scale electric power system. These global dynamics are broadly analogous to the dynamics of an idealized sand pile model that is expected to show SOC. This outline of a possible explanation of SOC in a power system shows the opposing forces that could give rise to a dynamic equilibrium with SOC properties. The opposing forces are, roughly speaking, the trends in load demands weakening parts of the system and the responses to blackouts strengthening parts of the system. It is interesting to reflect that responses to a blackout are usually regarded as an *outcome* of a detailed investigation of particular blackout causes. However, the more global view suggested here sees responses to blackouts as an *intrinsic part* of the global system dynamics.

3 PROGRESS IN FIRST YEAR

3.1 FIRST YEAR MAIN ACCOMPLISHMENTS

This section summarizes the main accomplishments in the first year of work. A detailed technical account of these accomplishments can be found in the papers reprinted in section 6. A summary of these accomplishments organized by project task can be found in section 3.2.

It is convenient to first list the three models used in the project so that they can be identified briefly in the sequel:

- **OPA model**. OPA is a software code to study self-organized criticality in power system blackouts. OPA models the cascading failures of the power system using DC load flow and LP dispatch and includes long term dynamics of load growth and power system improvement in response to blackouts. OPA was developed by ORNL, PSerc at Wisconsin and University of Alaska and is described in [Dobson01, Carreras01b] and section 6.1.

- **Hidden Failure model**. The hidden failure model is a software code to study the effect of relay misoperation in cascading failure blackouts. The hidden failure model represents relay misoperation as a function of line loading and uses DC load flow and LP dispatch. The hidden failure model was developed by PSerc at Cornell and is described in [Chen01] and section 6.2.

- **CASCADE model**. CASCADE is a simple analytically solvable model to study basic features of probabilistic cascading failure. CASCADE was developed by PSerc at Wisconsin and Cornell and is described in section 6.2.

The main accomplishments include:

- Increased understanding and development of the OPA model has yielded behavior with many features of self-organized criticality on artificial power networks and results with some similarity to the probability distributions of blackout sizes observed in real blackout data from North America. Key insights achieved are the discovery of two types of critical points in the model associated with generator and line limitations and the need to coordinate generator and line upgrades. [see section 6.1]

- The hypothesis that power systems show power law behavior and heavy tails in the distribution of blackout sizes near a certain critical loading has been tested with the OPA, Hidden Failure and CASCADE models. The results are broadly consistent with the hypothesis. The hypothesis is important for understanding how the operating decision of the power system loading level relates to greatly increased risk of large blackouts. [see section 6.2]

- Initial parameter sensitivity studies on the 176 bus WSCC system with the Hidden Failure model suggest how changes in spinning reserve, protection system improvements and prompt control by generation redispatch during cascading events affect the probability of large blackouts. [see section 6.3]

- Network size scaling studies with the OPA model have confirmed regions of power law behavior in the distribution of blackout sizes. [see section 6.1]

- The project has developed the CASCADE model to study basic features of probabilistic cascading failure and derived a formula for its probability distribution using combinatorial methods. CASCADE represents the progressive system weakening as the cascading outages proceed. [see section 6.2]

3.2 REPORT ON FIRST YEAR TASKS

This section summarizes the first year progress according to the planned tasks. All first year tasks have been substantially completed as detailed below.

Task 1: Improve global models of series of cascading failures.

(a) Clarify and develop representations of outages, overloads, and system memory between blackouts (Dobson, Carreras, Newman).

(b) Search for heuristics, theory and simplifications that can lead to better understanding (Carreras, Dobson, Thorp).

- We discovered that there are two types of blackouts occurring in the OPA model. One type involves line overloads and the other type involves generator overloads. Different types of critical behavior arise near these two system limits. Coordination of generator and line limits is important in the model and generator upgrade modeling has been reworked.
- We invented CASCADE, a new, analytically solvable model of probabilistic cascading failure that represents the progressive system weakening as the cascade proceeds.
- We developed a better understanding of extracting probability distribution data from the hidden failure model and improved the representation of multiply exposed lines.

Task 2: Implement global models in software

(a) Assess need for new LP solver to be able to simulate networks of more realistic size (Carreras, Dobson).

(b) Incorporate model improvements from Task 1(a) OR implement new LP solver from Task 2(a) (Carreras)

- We have tested three different LP solvers for serial machines. Of the three, the most effective and fastest one for this type of problem is the simplex method. Our standard calculations are done over 100000 days in order to gather enough statistical information on blackouts. For a network with 382 nodes with the fastest solver, this calculation takes about 4 weeks on a G-4 Macintosh computer. Therefore, the only way of handling larger networks would be by moving to a massively parallel computer with a parallel version of the LP-solver. This was not feasible within the constraints of the project budget.

- The modeling of generator upgrades from Task 1(a) has been developed and implemented in the OPA model.
- The improvement in the handling of multiply exposed lines has been coded into the Hidden Failure model.

Task 3: Develop test networks

(a) Finish data set for IEEE 118 bus network (Dobson).

(b) Set up WSCC system for input to OPA code (Dobson).

- Data sets for the IEEE 118 bus and 179 bus WSCC system networks have been created for the OPA code in the required format. Parameters may have to be adjusted to fine-tune the models.

Task 4: Study models by running software on test networks; develop diagnostics and analyze and interpret results

(a) Scaling studies of the blackout dynamics for different network sizes using current OPA model (Carreras).

(b) Parameter sensitivity studies on 176 bus WSCC system (Thorp)

(c) Investigate criticality as a function of loading in models without network improvements (Carreras, Dobson, Thorp).

- All these studies have been done and documented in section 6.

Task 5: Project first year report in November 2001

- This document is the project first year report. It includes planning for the second year tasks and is available in pdf format suitable for posting on a website.

3.3 PROJECT COORDINATION

The project team has a substantial history of productive collaboration and is producing results in close collaboration and papers with joint authorship [Carreras00, Carreras01a, Carreras01b, Carreras01c, Carreras02, Dobson01, Dobson02]. Coordination with Dr. David Newman at the Physics department in the University of Alaska-Fairbanks is ongoing. Ian Dobson spent a sabbatical year visiting Cornell University and worked with Jim Thorp on this project.

Team communication is a judicious combination of email, phone, and face to face meetings. There is a project web page hosted by PSerc at
http://www.pserc.wisc.edu/ecow/get/researchdo/certsdocum0/currentcer/
to log papers, presentations, and administration documents.

3.4 PAPERS AND PRESENTATIONS

The following two papers document in detail much of the technical progress on the project and are reprinted in section 6. The papers are in final form and can be posted on a web site in pdf format.

Dynamics, Criticality and Self-Organization in a Model for Blackouts in Power Transmission Systems, B.A. Carreras, V.E. Lynch, I. Dobson, and D.E. Newman. to appear at 35th Hawaii International Conference on System Sciences, Hawaii, January 2002. [see section 6.1]

Abstract: A model has been developed to study the global complex dynamics of a series of blackouts in power transmission systems [1, 2]. This model has included a simple level of self-organization by incorporating the growth of power demand and the engineering response to system failures. Two types of blackouts have been identified with different dynamical properties. One type of blackout involves loss of load due to lines reaching their load limits but no line outages. The second type of blackout is associated with multiple line outages. The dominance of one type of blackouts versus the other depends on operational conditions and the proximity of the system to one of its two critical points. The first critical point is characterized by operation with lines close to their line limits. The second critical point is characterized by the maximum in the fluctuations of the load demand being near the generator margin capability. The identification of this second critical point is an indication that the increase of the generator capability as a response to the increase of the load demand must be included in the dynamical model to achieve a higher degree of self-organization. When this is done, the model shows a probability distribution of blackout sizes with power tails similar to that observed in real blackout data from North America.

Examining Criticality of Blackouts in Power System Models with Cascading Events, I. Dobson, J. Chen, J.S. Thorp, B.A. Carreras, and D.E. Newman, to appear at 35th Hawaii International Conference on System Sciences, Hawaii, January 2002. [see section 6.2]

Abstract: As power system loading increases, larger blackouts due to cascading outages become more likely. We investigate a critical loading at which the average size of blackouts increases sharply to examine whether the probability distribution of blackout sizes shows the power tails observed in real blackout data. Three different models are used, including two simulations of cascading outages in electric power transmission systems. We also derive and use a new, analytically solvable model of probabilistic cascading failure which represents the progressive system weakening as the cascade proceeds.

The following five presentations were given:

Evidence for self-organized criticality in electric power blackouts, B. A. Carreras, D. E. Newman, I. Dobson, and A. B. Poole, 34rd Hawaii International Conference on System Sciences, Maui, Hawaii, January 2001.

Modeling blackout dynamics in power transmission networks with simple structure, B.A. Carreras, V.E. Lynch, M. L. Sachtjen, I. Dobson, D. E. Newman, 34th Hawaii International Conference on System Sciences, Maui, Hawaii, January 2001.

An initial model for complex dynamics in electric power system blackouts, I. Dobson, B. A. Carreras, V.E. Lynch, D. E. Newman, 34th Hawaii International Conference on System Sciences, Maui, Hawaii, January 2001.

Analysis of electric power system disturbance data, J. Chen, J.S. Thorp, M. Parashar, 34th Hawaii International Conference on System Sciences, Maui, Hawaii, January 2001.

Cascading failure and self-organized criticality in electric power system blackouts, I. Dobson, D.E. Newman, B.A. Carreras, and Vicki Lynch, NSF Workshop on Engineering the transport industries, Georgetown, Washington DC, August 13-14, 2001.

The following journal paper was submitted to the IEEE Transactions on power systems:

Evidence for self-organized criticality in a time series of electric power system blackouts, B. A. Carreras, D. E. Newman, I. Dobson, and A. B. Poole, preprint, submitted to IEEE Transactions on Power Systems, December 2001. [see section 6.4]

Abstract: We analyze a 15-year time series of North American electric power transmission system blackouts for evidence of self-organized criticality. The probability distribution functions of various measures of blackout size have a power tail and R/S analysis of the time series shows moderate long time correlations. Moreover, the same analysis applied to a time series from a sandpile model known to be self-organized critical gives results of the same form. Thus the blackout data is consistent with self-organized criticality. A qualitative explanation of complex dynamics observed in electric power system blackouts is suggested.

4 PLAN FOR SECOND YEAR WORK

The first year of the project concentrated on improving, implementing and understanding models capturing the complex dynamics of series of blackouts. These first year activities will be continued in the second year but emphasis will shift towards improving the realism of the models and data, trying to reproduce qualitative features of historical NERC data on blackouts, and assessing the prospects for controlling the complex model dynamics to mitigate or avoid large blackouts.

4.1 SECOND YEAR TASKS

The second year of project work builds on the first year tasks. The planned second year project tasks are shown below. There will be a project meeting of all the investigators at the HICSS meeting in January 2002 to revise the second year tasks if this is necessary in the light of the most recent progress and make more detailed plans and assignments. The revised plans will be documented in late January after the HICSS meeting.

Task 6: Apply improved global models to more realistic test networks and analyze and interpret results

(a) Studies using OPA model (Carreras)
(b) Studies using Hidden Failure model (Thorp)

Task 7: Refine data, modeling, algorithms, analysis and software to improve the results from task 6.

The main objective of task 7 is to reproduce and explain qualitative features of the historical NERC data on blackouts using the models developed by the project. Coordination between Wisconsin, ORNL and Cornell will be needed. The following task 7 subtasks will be revised in the light of the progress in the first year tasks.

(a) Implement model upgrades to efficiently compute larger networks
(b) Develop models, data sets, and analysis techniques as needed.
(c) Develop heuristics and theory that can lead to better understanding

Task 8: Report on any implications or insights for power system operation.

Assess the prospects for controlling the complex model dynamics to mitigate or avoid large blackouts. This task will require advice from David Newman of the University of Alaska-Fairbanks about general methods of control of complex systems near criticality.

Task 9: Draft final report in November 2002; final report finished January 2003

The draft final report will be circulated for comments to be included in the final version. The working title of the final report is "Complex systems approach to cascading failures." The final report will be produced in pdf format suitable for posting on a website.

4.2 DELIVERABLES

The deliverables for this project will include documented information in the form of technical papers. In addition, a final report will be prepared to include all of the details of the tasks.

4.3 PROJECT UNCERTAINTIES

1. Run time of model codes on large (greater than about 300 bus) networks is becoming excessive. Options for code upgrades to solve this are being explored.
2. Although the global models under development are simplified, they exhibit complicated behavior. The development of new insights and understanding of the models is very helpful for the project progress. Although good progress in understanding is being made and the research team caliber and expertise suggests that this good progress will continue, it is hard to schedule insights.
3. In general, the project is research pioneering an entirely new perspective on power system blackouts. Development of new models, analysis tools and insight is an iterative process. Because the work is novel, there is some uncertainty in estimating the difficulty of project tasks in advance.

4.4 BUDGET

B. A. Carreras and B. J. Kirby (ORNL)
$60,000 per year for 2 years, beginning Jan 1, 2001.

Ian Dobson (PSERC Wisconsin)
$40,000 per year for 2 years, beginning Jan 1, 2001.

Jim Thorp (PSERC Cornell)
$10,000 per year for 2 years, beginning Jan 1, 2001.

Work is approximately at 50% completion. Some carryover of funds into next fiscal year is anticipated to allow work in November-December 2001 to proceed. ORNL plans to carry over about $25,000.

5 REFERENCES

[Anderson96] P. M. Anderson, B. K. LaReverend, Industry experience with special protection schemes, IEEE Transactions on Power Systems, Vol. 11, No. 3, August 1996.

[Bak87] P. Bak, C. Tang and K Weisenfeld, self-organized criticality: an explanation of 1/f noise, Phys. Rev Lett. 59, 381 (1987).

[Bak93] P. Bak and K. Sneppen, Punctuated equilibrium and criticality in a simple model of evolution, Phys. Rev. Lett. **71**, 4083 (1993).

[Carlson94] J. M. Carlson, J. S. Langer, and B. E. Shaw, Dynamics of earthquake faults, Rev. Modern Phys. **66** (2), 657-70 (1994).

[Carreras96] B. A. Carreras, D. E. Newman, V. E. Lynch, and P. H. Diamond, A model realization of self-organized criticality for plasma confinement, Phys. Plasmas **3**, 2903 (1996).

[Carreras98a] B. A. Carreras, B. van Milligen, M. A. Pedrosa, R. Balbín, C. Hidalgo, D. E. Newman, E. Sánchez, M. Frances, I. García-Cortés, J. Bleuel, M. Endler, S. Davies, and G. F. Matthews, Long-range correlations in plasma edge turbulence, Phys. Rev. Lett. 80 (20), 4438-4441 (1998).

[Carreras99] B. A. Carreras, B. Ph. van Milligen, M. A. Pedrosa, R. Balbin, C. Hidalgo, D. E. Newman et al, Experimental evidence of long-range correlations and self-similarity in plasma fluctuations, Physics of Plasmas 6 (5): 1885-1892 Part 2 May 1999.

[Carreras00] B. A. Carreras, D. E. Newman, I. Dobson, and A. B. Poole, Initial evidence for self-organized criticality in electric power blackouts, 33rd Hawaii International Conference on System Sciences, Maui, Hawaii, Jan. 2000.

[Carreras01a] B. A. Carreras, D. E. Newman, I. Dobson, and A. B. Poole, Evidence for self-organized criticality in electric power blackouts, 34rd Hawaii International Conference on System Sciences, Maui, Hawaii, Jan. 2001.

[Carreras01b] B.A. Carreras, V.E. Lynch, M. L. Sachtjen, I. Dobson, D. E. Newman, Modeling blackout dynamics in power transmission networks with simple structure, 34th Hawaii International Conference on System Sciences, Maui, Hawaii, Jan. 2001.

[Carreras01c] B. A. Carreras, D. E. Newman, I. Dobson, and A. B. Poole, Evidence for self-organized criticality in a time series of electric power system blackouts, preprint, submitted to IEEE Transactions on Power Systems, December 2001.

[Carreras02] B.A. Carreras, V.E. Lynch, I. Dobson, D.E. Newman, Dynamics, criticality and self-organization in a model for blackouts in power transmission systems, Thirty-fifth Hawaii International Conference on System Sciences, Hawaii, January 2002.

[Chen01] J. Chen, J.S. Thorp, M. Parashar, Analysis of electric power system disturbance data, 34th Hawaii International Conference on System Sciences, Maui, Hawaii, Jan. 2001.

[Dobson01] I. Dobson, B. A. Carreras, V.E. Lynch, D. E. Newman, An initial model for complex dynamics in electric power system blackouts, 34th Hawaii International Conference on System Sciences, Maui, Hawaii, Jan. 2001.

[Dobson02] I. Dobson, J. Chen, J.S. Thorp, B.A. Carreras, D.E. Newman, Examining criticality of blackouts in power system models with cascading events, Thirty-fifth Hawaii International Conference on System Sciences, Hawaii, January 2002.

[Drossel92] B. Drossel and F. Schwabl, Self-organized critical forest-fire model, Phys Rev. Lett. **69**, 1629 (1992).

[Hurst51] H. E. Hurst, Long-term storage capacity of reservoirs, Trans. Am. Soc. Civil Eng. **116,** 770 (1951).

[Hwa92] T. Hwa and M. Kadar, Avalanches, hydrodynamics, and discharge events in models of sandpiles, Phys. Rev A **45**, 7002 (1992).

[Kadanoff89] L. P. Kadanoff, S. R. Nagel, L. Wu and S-M. Zhou; Scaling and universality in avalanches, Phys. Rev. A 39, 6524 (1989)

[Leland94] W. E. Leland, M. S. Taqqu, W. Willinger, and D. V. Wilson, "On the self-similar nature of ethernet traffic," IEEE/ACM Transaction on Networking, vol. 2, pp. 1-15, (1994).

[Lo91] Lo, A. W., Long-term memory in stock market prices, Econometrica **59** (5): 1279-1313. (1991).

[Mandelbrot69a] B. B. Mandelbrot and J. R. Wallis, Noah, Joseph, and operational hydrology, Water Resources Research **4,** 909-918 (1969).

[Mandelbrot69b] B. B. Mandelbrot and J. R. Wallis, Some long-run properties of geophysical records, Water Resources Research **5,** 422-437 (1969).

[Mantegna95] R. N. Mantegna and H. E. Stanley, Scaling behaviour in the dynamics of an economic index, Nature **376**, 46 (1995).

[Mantegna94] R. N. Mantegna and H. E. Stanley, Stochastic process with ultraslow convergence to a Gaussian: the truncated Levy flight, Phys. Rev. Lett. **73**, 2946 (1994).

[Nagel95] K. Nagel and M. Paczuski, Emergent traffic jams, Phys. Rev. E 51, 2909 (1995).

[Newman96a] D. E. Newman, B. A. Carreras, P. H. Diamond and T. S. Hahm, The dynamics of marginality and self-organized criticality as a paradigm for turbulent transport, Phys. Plasmas **3** (5), May (1996).

[Newman96b] D. E. Newman, B. A. Carreras and P. H. Diamond, Sandpile dynamics as a paradigm for turbulent transport, pp. 307-321 in Transport Chaos and Plasma Physics 2, Eds. S. Benkadda, F. Doveil, and Y. Elskens, World Scientific, Singapore, (1996).

[Newman96c] D. E. Newman, B. A. Carreras, and P. H. Diamond, The dynamics of sandpiles with sheared flow, Phys. Letters A **218**, 58 (1996).

[Newman98] D. E. Newman, B. A. Carreras, and Haiyin Chen, Triggering large events in self organized critical systems, submitted to Phys Rev Letters (1998).

[Sachtjen00] Sachtjen ML, Carreras BA, Lynch VE, Disturbances in a power transmission system, PHYS REV E 61 (5): 4877-4882 Part A May 2000.

[Thorp98] J. S. Thorp, A. G. Phadke, S. H. Horowitz, S. Tamronglak, Anatomy of power system disturbances: importance sampling, International journal of electrical power & energy systems 20: (2) 147-152 Feb 1998.

[Thorp01] J. S. Thorp, H. Wang, Computer simulation of cascading disturbances in electric power systems; impact of protection systems on transmission system reliability, Final report, Power Systems Engineering Research Center, PSerc publication 01-01, May 2001, available from http://www.pserc.wisc.edu/.

6 TECHNICAL PAPERS

6.1 Dynamics, criticality and self-organization in a model for blackouts in power transmission systems

B.A. Carreras, V.E. Lynch, I. Dobson, D.E. Newman

© 2002 IEEE. Reprinted, with permission, from

Thirty-fifth Hawaii International Conference on System Sciences, Hawaii, January 2002.

Hawaii International Conference on Systems Sciences, January 2002, Hawaii. © IEEE

Dynamics, Criticality and Self-organization in a Model for Blackouts in Power Transmission Systems

B. A. Carreras
Oak Ridge National Laboratory
Oak Ridge, TN 37831
carrerasba@ornl.gov

V. E. Lynch
Oak Ridge National Laboratory
Oak Ridge, TN 37831
lynchve@ornl.gov

I. Dobson
ECE Dept., University of Wisconsin
Madison, WI 53706 USA
dobson@engr.wisc.edu

D. E. Newman
Physics Dept., University of Alaska
Fairbanks, AK 99775 USA
ffden@uaf.edu

Abstract

A model has been developed to study the global complex dynamics of a series of blackouts in power transmission systems [1, 2]. This model has included a simple level of self-organization by incorporating the growth of power demand and the engineering response to system failures. Two types of blackouts have been identified with different dynamical properties. One type of blackout involves loss of load due to lines reaching their load limits but no line outages. The second type of blackout is associated with multiple line outages. The dominance of one type of blackouts versus the other depends on operational conditions and the proximity of the system to one of its two critical points. The first critical point is characterized by operation with lines close to their line limits. The second critical point is characterized by the maximum in the fluctuations of the load demand being near the generator margin capability. The identification of this second critical point is an indication that the increase of the generator capability as a response to the increase of the load demand must be included in the dynamical model to achieve a higher degree of self-organization. When this is done, the model shows a probability distribution of blackout sizes with power tails similar to that observed in real blackout data from North America.

1. Introduction

The first version of the ORNL-PSerc-Alaska (OPA) model of series of blackouts in power system transmission systems was proposed in [1, 2]. This first version of the OPA model showed how the slow opposing forces of load growth and network upgrades in response to blackouts could self organize the power system to dynamic equilibrium. Blackouts were modeled by overloads and outages of lines determined in the context of LP dispatch of a DC load flow model. This model showed complex dynamical behaviors and has a variety of transition points as a function of increasing power demand [3]. Some of these transition points have the characteristic properties of a critical transition. That is, when the power demand is close to a critical value, the probability distribution function (PDF) of the blackout size has an algebraic tail and across the critical point the system changes sharply. One such consequence of the critical transition is that at these transition points, the power served is maximum and the risk for blackouts increases sharply. This fast variation near the critical point is illustrated in Fig. 1. Therefore, it may be natural for power transmission systems to operate close to and somewhat below those points.

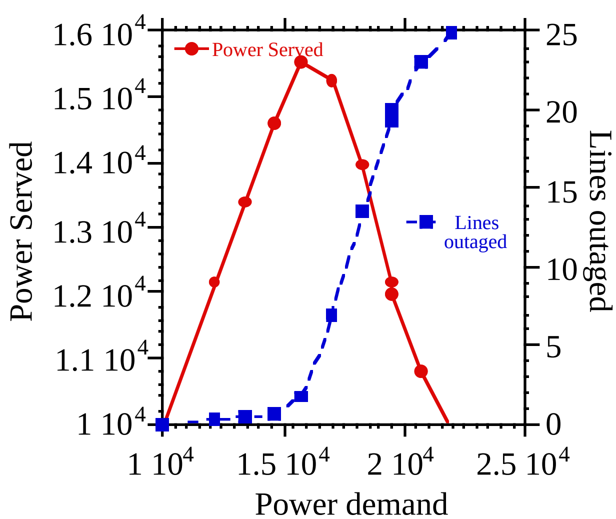

Fig. 1. Power served and number of lines outage for a tree network with 190 nodes as a function of the power demand.

The fact that, on one hand, there are critical points with maximum power served and, on the other hand, there is a self-organization process that tries to maximize efficiency and minimize risk may lead to a power transmission model governed by self-organized criticality (SOC) [4].

The operation of power transmission systems results from a complex dynamical process in which a diversity of opposing forces regulate both the maximum capabilities of the system components and the loadings at which they operate. These forces enter in a highly nonlinear manner and may cause a self-organization process to be ultimately responsible for the regulation of the system. This view of a power transmission system considers not only the engineering and physical aspects of the power system, but also the engineering, economic, regulatory and political responses to blackouts and increases in load power demand. A detailed incorporation of all these aspects of the dynamics into a single model would be extremely complicated if not intractable due to the human interactions involved. However, it is useful to consider simplified models with some approximate overall representation of the opposing forces in order to gain some understanding of the complex dynamics in such a self-organized framework and the consequences for power system planning and operation.

The OPA model is motivated by analyses of NERC data that indicate power tails in the probability distribution of the size of North American blackouts [5,7]. (Power tails decay as according to a power law and are also exhibited by complex systems near criticality.) These observations indicate the non-Gaussian character of the blackout size probability distributions and are of concern because they indicate a much larger risk of large blackouts than might be expected. Confirming and understanding this power dependence in the probability distribution tails is of course very important in doing any risk analysis of power systems.

Note that transition points are essentially determined from power systems physics and engineering constraints, however, the dynamical evolution involves aspects that are less clearly defined by simple deterministic rules. These components of the model may be developed at different levels of complexity representing different approximations to the "real" system.

The main purpose of the OPA model is to study the complex behavior of the dynamics of series of blackouts. In this paper we examine critical points of the OPA model to understand them better. This understanding allows us to extend the modeling of the self-organization of the system to represent generator upgrades as well as network upgrades. With this improvement to the OPA model, we demonstrate self-organization of the system to a critical point at which the probability distribution of blackout size resembles the probability distribution of the NERC data.

2. OPA fast dynamics blackout model

In the OPA model of [1,2], the dynamics involves two intrinsic time scales. There is a slow time scale, of the order of days to years, over which load power demand slowly increases and the network is upgraded in engineering responses to blackouts. These slow opposing forces of load increase and network upgrade self organize the system to a dynamic equilibrium. These slow dynamics are summarized in Appendix I. There is also a fast time scale, of the order of minutes to hours, over which cascading overloads or outages may lead to blackout.

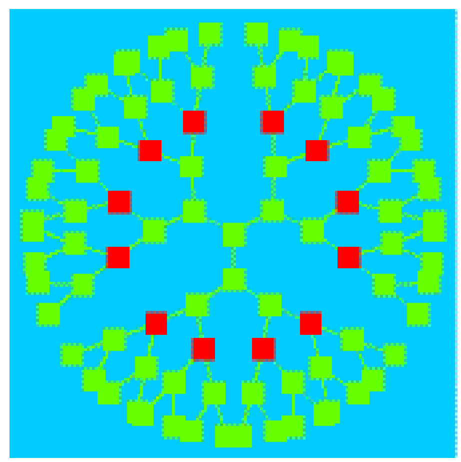

Fig. 2. A 94-node tree network with 12 generators and 82 loads.

To investigate the critical points of the OPA model in section 3, we suppress the modeling of the slow dynamics responsible for the self-organization and study only the fast dynamics of the blackouts. That is, we fix the network by suppressing the network upgrades and treat the load demands as deterministic or random parameters to be specified as inputs to the model. This section explains the fast dynamics of the OPA model.

In this paper, we investigate the blackout dynamical model applied to ideal grid networks that have a tree structure. An example of a tree network with 94 nodes is shown in Fig. 2.

In any network, the network nodes (buses) are either loads (L) (gray squares in Fig. 2), or generators (G), (black squares in Fig. 2). The power P_i injected at each node is positive for generators and negative for loads, and the maximum power injected is $P_i^{\max}$. The transmission line connecting nodes i and j has power flow F_{ij}, maximum power flow $F_{ij}^{\max}$, and the impedance of the line z_{ij}. There are $N_N = N_G + N_L$ total nodes and N_l lines, where N_G is the number of generators and N_L is the number of loads.

The blackout model is based on the standard DC power flow equation,

$$F = AP \tag{1}$$

where F is a vector whose N_L components are the power flows through the lines, F_{ij}, P is a vector whose N_N–1 components are the power of each node, P_i, with the exception of the reference generator, P_0, and A is a constant matrix. The reference generator power is not included in the vector P to avoid singularity of A as a consequence of the overall power balance.

The input power demands are either specified deterministically or as an average value plus some random fluctuation around the average value. The random fluctuation is applied to either each individual load or to "regional" groups of load nodes.

The generator power dispatch is solved using standard LP methods. Using the input power demand, we solve the power flow equations, Eq. (1), with the condition of minimizing the following cost function:

$$\text{Cost} = \sum_{i\in G} P_i(t) - W \sum_{j\in L} P_j(t) \tag{2}$$

We assume that all generators run at the same cost and all loads have the same priority to be served. However, we set up a high price for load shed by setting W = 100. This minimization is done with the following constraints:

1) Generator power $\quad 0 \le P_i \le P_i^{\max} \quad i \in G$
2) Load power $\quad P_j \le 0 \quad j \in L$
3) Power flows $\quad \left|F_{ij}\right| \le F_{ij}^{\max}$
4) Power balance $\quad \sum_{i\in G\cup L} P_i = 0$

This linear programming problem is numerically solved using the simplex method as implemented in [6]. The assumption of uniform cost and load priority can of course be relaxed but changes to the underlying dynamics are not likely from this.

In solving the power dispatch problem for low load power demands, the initial conditions are chosen in such a way that a feasible solution of the linear programming problem exists. That is, the initial conditions yield a solution without line overloads and without power shed. Increases in the average load powers and random load fluctuations can cause a solution of the linear programming with line overloads or requires load power to be shed. At this point, a cascading event may be triggered.

A cascading overload may start if one or more lines are overloaded in the solution of the linear programming problem. We consider a line overloaded if the power flow through this line is within 1% of $F_{ij}^{\max}$. At this point, we assume that there is a probability p_2 that an overloaded line will outage. If an overloaded line outages, we reduce its corresponding $F_{ij}^{\max}$ by large amount (making it effectively zero) to simulate the outage, and a new solution is calculated. This process can require multiple iterations and continues until a solution is found with no more outages.

This fast dynamics model does not attempt to capture the intricate details of particular blackouts, which may have a large variety of complicated interacting processes also involving, for example, protection systems, dynamics and human factors. However, the fast dynamics model does represent cascading overloads and outages that are consistent with some basic network and operational constraints.

Calculations with the fast dynamics model are carried out by slowly increasing the average load demands over 10^5 iterations. If one regards each model run as occurring at successive peak daily loads (when blackouts are most likely), then this corresponds to an average load demand increasing slowly in a power network under fixed conditions over a period of 10^5 days. This is not because we try to simulate a real power transmission network, as this time scale is too long for the power system remaining under the same rules and conditions. Rather it is done in order to accumulate the necessary statistics to calculate the PDFs and other statistical measures needed to understand the system and ultimately do risk analysis. This emphasizes the problem of working with real data [5,7], which has only been available for a period of time more than an order of magnitude shorter than the time used in these calculations.

3. Critical points of the OPA fast dynamics blackout model

This section studies the behavior of blackouts in the fast dynamics model of section 2 as the average load demand is increased. As the power demand increases, we found several transition points. Some of these transition points have the characteristic properties of a critical transition. That is, when the load power demand is close to a critical value, the probability distribution function (PDF) of the blackout size has an algebraic tail and at the critical loading the risk for blackouts increases sharply. In particular, there is a sudden change in the rate of change of load shed as a function of the power demand. These transitions are caused by limits in the power system and they can be grouped in two types of limiting conditions:

1. Limits set by the available power generation.
2. Limits set by the transmission capacity of the grid.

An example with two of these limits is shown in Fig. 3. For a tree network with 382 nodes (12 generators and 370 loads), we increase power demand by increasing all loads at the same rate. The load demand in this example is deterministic and there is no random fluctuation in the load demands. As we reach a power demand of 31480, the total generator capacity, load power shedding starts. As the demand continues to increase, all power above 31480 is shed. When the demand reaches 45725, the power flow in some lines reaches the line power flow limit and some line outages are produced. This causes a further increase in the load power shed.

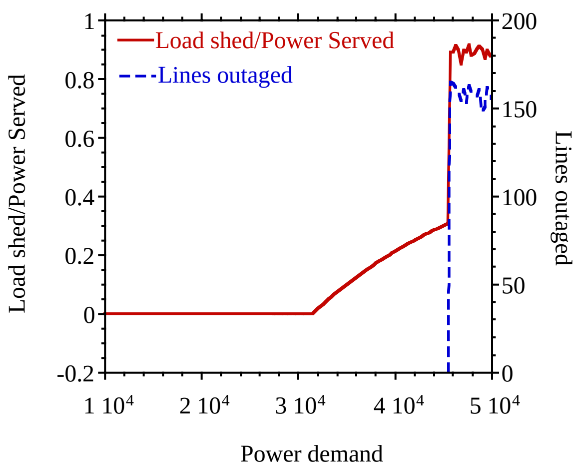

Fig. 3. Normalized power shed and number of outaged lines for a tree network with 382 nodes as a function of power demand.

Why is there a second transition after the total power served is kept constant that is therefore independent of the level of demand? The reason is that the individual loads increase and the power shed is not uniform over all loads. Therefore, even if the total power served is constant, the power delivered to some of the loads is increased as the total demand increases and that leads to overloading lines and possible line outages. The second transition point occurs at the same value of the power demand even in the absence of the first critical point, because it depends on the power of individual loads and the maximum power flow that the lines connecting them can carry. These results come from studying a sequence of cases under the same conditions but without random load fluctuations. The important point is that the first transition point is a function of the total power demand, while the second depends on the local value of the loads near the lines that are closer to overload.

Some of these transition points have the characteristic properties of a critical transition. For the calculation shown in Fig. 3, we have used the power demand as control parameter and we have done a scan starting with all load nodes having the same power loads and not allowing for fluctuations. Clearly the power generation limit (the first inflection point in the load-shed curve in Fig. 3) behaves as a second order transition point, characterized by a continuous function with discontinuous derivative. The critical point in this case is given by the generator power margin reaching zero, that is $\Delta P \equiv \sum_{i \in G} P_i - P_{Demand} = 0$. The load shed is a continuous function of the load power demand, but its derivative with respect to the load power demand is discontinuous at the transition point.

In the proximity of the generator critical point, the PDF of the normalized load shed has an algebraic tail. To calculate the PDF, we have to introduce noise into the system and this is done by introducing random fluctuations of the load power demands. The load fluctuations are controlled by the parameter γ described in Appendix I. For a given value of γ, the average fluctuation induced in the total power demand is $(\gamma - 1)/(2\sqrt{N_L})$. Therefore, we can also use the parameter γ as a control parameter to scan over the critical point.

For the sequence of results in Fig. 4, the first critical point is reached with $\gamma = 1.35$. This corresponds to an averaged fluctuation in the power demand of 10%. As γ increases, more of the fluctuations in power demand reach the critical point, and the PDF of the normalized load shed develops an algebraic tail with decay index close to –1. Above the critical point, the PDF changes to an exponential tail. This is shown in Fig. 4 for a 94-node tree network. We have chosen network conditions with the generator power limit well below the limits set by the transmission lines in order to avoid interacting with the line limits critical point. In this case, we have given an averaged value to the generation margin capability of 5% and varied the maximum daily oscillation of the loads. Naturally, in this situation there are no outages in the system and power shedding is simply due to a supply shortage.

The second transition point in Fig. 3 is associated with line limits and is more difficult to characterize. To identify this transition point, it is useful to define the fraction of overload for a given line as

$$M_{ij} = \frac{F_{ij}}{F_{ij}^{\max}} \tag{3}$$

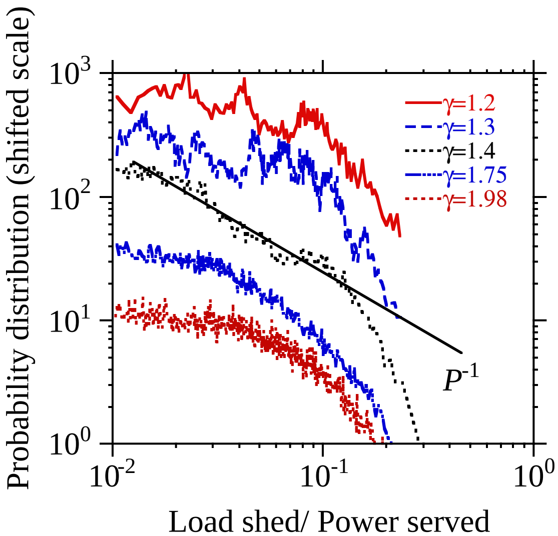

Fig. 4. PDF of the normalized load shed for a tree 94-node tree network for different levels of the load fluctuations.

We can then calculate $M_{\max} \equiv \max_{ij} M_{ij}$. The second transition point in Fig. 3 is given by $M_{\max} = 1$. The properties of this type of transition point depend on the value of the parameter p_2, the probability that an overloaded line outages. Of course, if $p_2 = 0$, there are no line outages and this transition point has similar properties as the generator limit, and looks like a second order transition. However, for $p_2 = 1$, all overload lines outage. This is the value of p_2 used in the calculation shown in Fig. 3 and the transition point has some of the features of a first order transition characterized by a discontinuous jump in the function. In Fig. 5, we show examples of transitions for these different values of the relevant parameters. For values of p_2 between 0 and 1, we have intermediate situations that are more difficult to characterize. Only for $p_2 = 0$ does the PDF of the load shed near the critical point have a clear algebraic tail.

The full classification of the properties of these transition points for all values of the parameters is beyond the scope of this paper.

In trying to describe the realistic dynamics of power transmission systems, it is found that the best choice of parameters is when both critical points are close to each other. In this case, we can combine the existence of power tail in the PDF of the load shed with the presence of outages.

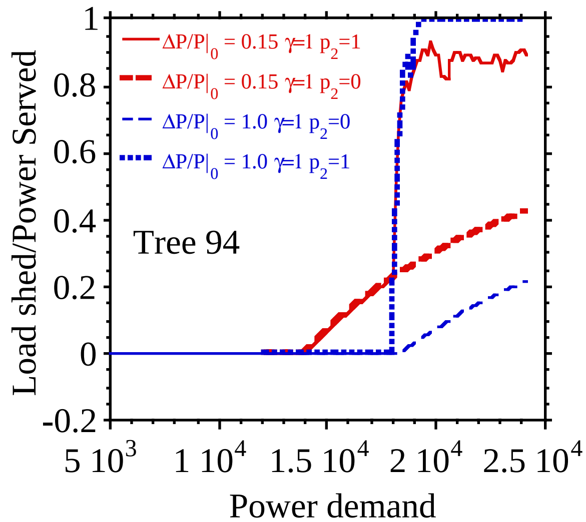

Fig. 5. Normalized power shed for a tree network with 94 nodes as a function of load power demand. Four different scenarios are included.

4. Self-organization dynamics

To transform the model described in Section 2 into a self-organized dynamical system we must include some of the opposing forces that act on the power transmission system. One example of these opposing forces is the growth of the demand and the system response through upgrading the system. These opposing mechanisms were incorporated in the model in Refs. [1, 2] and a short description of this model is given in the Appendix I. In this model, all loads are multiplied by a fixed constant $\gamma > 1$ at the start of the day. This causes an exponential increase in the average load demand. The generator capabilities are incremented in the same way; therefore, the generator limits are never reached in this model. The response mechanism was triggered by the blackout outages. When there is a blackout, the overload lines have their limits incremented by multiplying them by $\mu > 1$. The combined effect of these slow dynamics is that the system self-organizes close to the critical point of the outages (second point in the example of Fig. 3).

In order to have a self-organization mechanism that includes the growth of maximum generator power, we have used tested several algorithms. One of the simplest forms incorporating such a mechanism is based on the increase of maximum generator power as a response to the load demand. We have limited the model to increases in maximum generator power at the same nodes that initially had generators. In doing so, we have implemented the following rules:

a. The increase in power is quantized. This may reflect the upgrade of a power plant or adding generators. We have tried two possibilities. The increase is taken to be either a fixed quantity or a fixed ratio to the total power. The second approach seems to work better, in the sense of convergence to a steady state. Therefore, we introduce the quantity

$$\Delta P_a \equiv \kappa\left(P_T / N_G\right) \qquad (4)$$

Here, P_T is the total power demand, N_G is the number of generator nodes, and κ is a parameter that we have taken to be a few percent.

b. To be able to increase the maximum power in node j, the sum of the power flow limits of the lines connected to j should be 20% larger than the existing generating power plus the addition at node j. The 20% value is an arbitrary quantity that provides a safety margin so that the line ratings are coordinated with the generator capabilities.

c. A second condition to be verified before any maximum generator power increase is that the mean generator power margin has reached a threshold value. That is, we define the mean generator power margin at a time t as:

$$\frac{\Delta P}{P} = \frac{\sum_{j \in G} P_j - P_0 e^{\lambda t}}{P_0 e^{\lambda t}} \qquad (5)$$

where P_0 is the initial power load demand.

d. Once condition c) is verified, we choose a node at random to test condition b). If the chosen node verifies condition b), we increase its power by the amount given by Eq. (4). If condition b is not verified, we choose another node at random and iterate. After power has been added to a node, we recalculate the mean generator power margin, Eq. (5), and continue the process till $\Delta P/P$ is above the prescribed quantity. This is motivated by the fact that utilities are, in general, likely to build a power plant where the transmission capacity already exists.

This algorithm seems to provide the self-organization process that we were looking for in the following sense. The maximum generator power stays close to and below the critical point, which results in PDFs with power law tails. The new measure of criticality is the mean generator power margin and this quantity converges to a steady state in a reasonable amount of time. Its mean values is approximately

$$\left\langle \frac{\Delta P}{P} \right\rangle = \left.\frac{\Delta P}{P}\right|_{threshold} - \frac{\kappa}{2N_G}. \qquad (6)$$

This result is reasonable because only one node gets an increase at a given time.

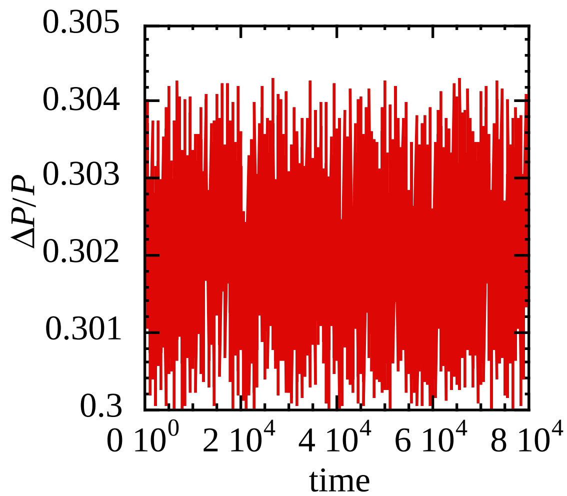

Fig. 6. Time evolution of $\Delta P/P$ for a case with κ = 0.04, threshold $\Delta P/P$ = 0.3.

It is also possible to introduce a time delay between the detection of a limit in the generation margin and the increase of the maximum generator power. This delay would represent the construction time. However, the result is the same as increasing the value of κ in Eq. (4), which can also give an alternative interpretation for κ.

In Fig. 6, we have plotted an example of time evolution of the generator margin $\Delta P/P$ for a case with κ = 0.04, threshold $\Delta P/P$ = 0.3, and 10 generator nodes. Increasing κ gives larger oscillations. The results, characterized by the PDF of the normalized power shed, do not seem to depend on the particular value of κ. They do depend on the value taken for the threshold of $\Delta P/P$. If the latter is not the critical value, we do not get critical behavior, as expected. Note that the critical value for $\Delta P/P$ is a function of the maximum oscillation of the power load as described in Section 3.

Once we have determined from the load scans of Section 3 what the critical points are, we can explore the dynamics of self-organization. In combining the two dynamical loops, the real self-organized critical point that the system is operating near is the point where the two types of critical points are close to each other. Therefore, both the line improvement and the generator upgrade in the dynamics of the system are needed in the dynamical evolution. Once we have both of them together, the PDFs of the power shed have well-developed power tails. This is shown in Fig. 7, where the PDF of the load shed normalized to the total power demand for three different tree configurations has been plotted.

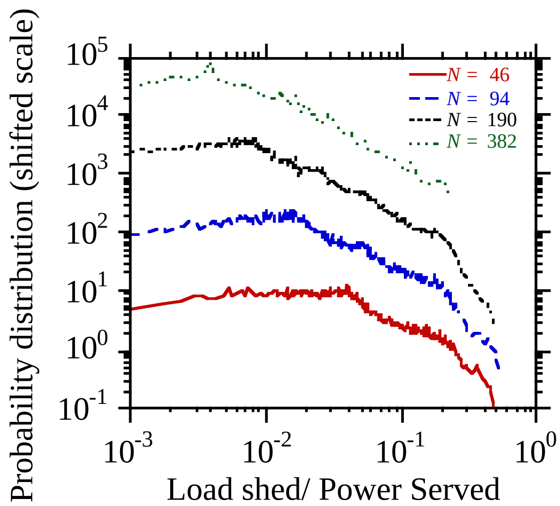

Fig. 7. PDF of the load shed normalized to the total power demand for four different tree networks.

The power-law-scaling region increases with the number of nodes in the network. The power decay index is practically the same for the four networks and close to –1.0. The particular values of the decay index for each network are given in Table I.

The range of the power tail region is defined as the ratio of the maximum and minimum load shed described by the power law. From the values obtained for the four networks listed in Table I, we can see that the range scales with the network size.

Table I

Number of nodes	PDF decay index	Range of power tail
46	-1.13	7
94	-1.16	17
190	-1.16	36
382	-1.21	62

The PDFs plotted in Fig. 7 are very similar to the PDFs of the normalized load shed obtained by direct power demand scan near the critical points with an important difference that they are now self organized.

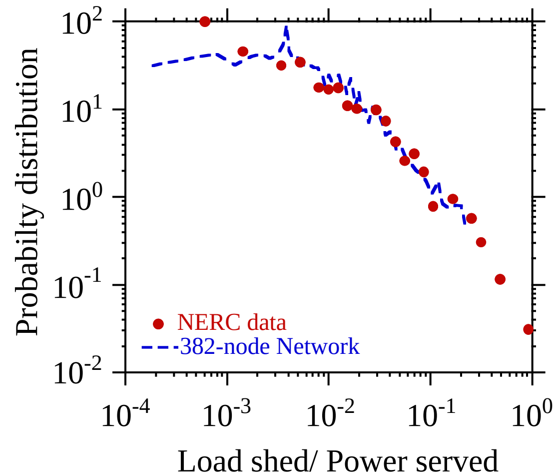

Fig. 8. PDF of the normalized load shed for the 382-node tree network and for the North American blackouts in 15 years of NERC data normalized to the largest size blackout

The form of these PDFs, or at least their power tail, seems to have a universal character. Therefore, we can try to compare the PDF of the normalized load shed obtained for the largest network with the PDF of the blackouts obtained in the analysis of the data from the last 15 years in the U.S. We have plotted the latter normalizing the events to the largest value over this period of time.

The level of agreement between the power tails of these two PDFs is remarkable. This seems to indicate that the dynamical model for the blackout has captured some of the main features of the data.

5. Discussion and conclusions

The opposing forces organizing the system, which in this paper are crudely represented by load demand increases and upgrades to network and generation capacity, may also be seen as the outcomes of design and operational procedures that trade off system security (risk of blackout) and maximizing the energy or peak power delivered. It is not clear how the self-organization we model is divided between design and planning procedures and operational procedures. In power system design and planning, design rules can incorporate previous experience of blackouts or designs may be tested by extensive simulations. In operations, real blackouts do of course occur and have significant impacts on operation, upgrades and repair, but there are also engineering responses to simulated events. A key question addressed but not fully answered in this paper, assumes from the power tails observed in the NERC data that North American power systems have been operated near a critical point and asks why or how this arises. Operational security criteria such as the n-1 criterion do influence the power system loading and planning, as well as the probability of cascading outages, and it would be interesting to determine the extent to which application of these criteria would lead to operation of the system near critical loading at peak load. That is, do specific security criteria contribute to self-organization to criticality? A fundamental understanding of the relation between security criteria and the risk or distribution of blackouts is particularly needed as the tested practices of the past are changed to accommodate deregulated power systems.

To understand the complex dynamics of series of blackouts in power systems, we proposed the OPA model. The OPA model incorporated a simple level of self-organization by including the growth of the load power demand and the engineering response to system failures. This model shows a variety of possible transition points, some linked to line outages in the system and others linked to the limits in the generation capacity. We have found that critical behavior emerges when these transition points correspond to similar power demand levels. Close to this critical point, the system reaches a maximum capacity for power transmission and the PDF of the blackout sizes have a power tail.

For the system to self-organize near to this critical point, we have to model the dynamics of the upgrading of the generator capacity as a response to the increased load demand. This leads to a double response loop in the model: 1) line upgrades and 2) generator upgrades. Under these conditions, the model has the characteristic properties of a system governed by self-organized criticality. The PDF of the blackouts size has the same power dependence that have been found from the analysis of NERC data for the North American power grid over a period of 15 years.

In these studies, we have limited the application of the model to idealized power grid systems with tree structure. Applications to more realistic power networks are under way.

Acknowledgement

Part of this research has been carried out at Oak Ridge National Laboratory, managed by UT-Battelle, LLC, for the U.S. Department of Energy under contract number DE-AC05-00OR22725. Ian Dobson and David Newman gratefully acknowledge support in part from NSF grants ECS–0085711 and ECS–0085647. Ian Dobson and B. A. Carreras gratefully acknowledge coordination of part of this work by the Consortium for Electric Reliability Technology Solutions and funding in part by the Assistant Secretary for Energy Efficiency and Renewable Energy, Office of Power Technologies, Transmission Reliability Program of the U.S. Department of Energy under contract 9908935 and Interagency Agreement DE-A1099EE35075 with the National Science Foundation.

Appendix I: Slow dynamics of load increase and network upgrade in OPA model.

The slow dynamics proposed in [1, 2] model the growth of the demand and response to the blackout by upgrades in the grid transmission capability. The slow dynamics is carried out by a simple set of rules. At the beginning of the day *t*, we apply the following rules:

1. Growth of the power demand. All loads are multiplied by a fixed parameter λ that represents the daily rate of increase in electricity demand. On the bases of the past electricity consumption, we had estimated that λ = 1.00005. This value corresponds to a yearly rate of 1.8%.

   $$P_i(t) = \lambda P_i(t-1) \quad \text{for } i \ni L \qquad \text{(AI-1)}$$

   Equally, the maximum generator power is increased at the same rate

   $$P_i^{\max}(t) = \lambda P_i^{\max}(t-1) \quad \text{for } i \ni G \qquad \text{(AI-2)}$$

2. Power transmission grid improvement. We assume a gradual improvement in the transmission capacity of the grid in response to the outages and blackouts. This improvement is implemented through an increase of $F_{ij}^{\max}$ for the lines that have overload during a blackout. That is.

   $$F_{ij}^{\max}(t) = \mu F_{ij}^{\max}(t-1) \qquad \text{(AI-3)}$$

   if the line *ij* overloads during a blackout. We take μ to be a constant and this parameter is the main control parameter in this system
3. Daily power fluctuations. To represent the daily local fluctuations on power demand, all power loads are multiplied by a random number *r*, such that $1/\gamma \le r \le \gamma$. We generally choose γ in the range 1 to 1.4. We also assign a probability for a random outage of a line. We represent a line outage by multiplying its impedance by a large number κ_1 and dividing its corresponding $F_{ij}^{\max}$ by another large

number κ_2. In the present calculations, these numbers are of the order of 1000.

After applying these three rules to the network parameters, we look for a solution of the power flow problem using linear programming as described in section 2.

References

[1] I. Dobson, B.A. Carreras, V. Lynch, D.E. Newman, An initial model for complex dynamics in electric power system blackouts, 34th Hawaii International Conference on System Sciences, Maui, Hawaii, January 2001.

[2] B.A. Carreras, V.E. Lynch, M. L. Sachtjen, I. Dobson, D.E. Newman, Modeling blackout dynamics in power transmission networks with simple structure, 34th Hawaii International Conference on System Sciences, Maui, Hawaii, January 2001.

[3] I. Dobson, J. Chen, J.S. Thorp, B.A. Carreras, D.E. Newman, Examining criticality of blackouts in power system models with cascading events, 35th Hawaii International Conference on System Sciences, Hawaii, January 2002.

[4] P. Bak, C. Tang, and K. Wiesenfeld, "Self-Organized Criticality: An Explanation of 1/f Noise," *Phys. Rev. Lett.* **59**, 1987, pp. 381-4.

[5] B.A. Carreras, D.E. Newman, I. Dobson, and A.B. Poole, Evidence for self-organized criticality in electric power blackouts," 34th Hawaii International Conference on System Sciences, Maui, Hawaii, 2001

[6] W.H. Press, B.P. Flannery, S.A. Teukolsky, and W. T. Vetterling, "Numerical recipes in C," Cambridge University Press, Cambridge, 1988.

[7] J. Chen, J.S. Thorp, M. Parashar, Analysis of electric power disturbance data, 34th Hawaii International Conference on System Sciences, Maui, Hawaii, January 2001.

6.2 Examining criticality of blackouts in power system models with cascading events

I. Dobson, J. Chen, J.S. Thorp, B.A. Carreras, D.E. Newman

© 2002 IEEE. Reprinted, with permission, from

Thirty-fifth Hawaii International Conference on System Sciences, Hawaii, January 2002.

Hawaii International Conference on System Sciences, January 2002, Hawaii. © 2002 IEEE.

Examining criticality of blackouts in power system models with cascading events

I. Dobson
ECE Department
Univ. of Wisconsin
Madison WI 53706
dobson@engr.wisc.edu

J. Chen J.S. Thorp
School of ECE
Cornell University
Ithaca NY 14850
thorp@ee.cornell.edu

B.A. Carreras
Oak Ridge National Laboratory
Oak Ridge TN 37831
carrerasba@ornl.gov

D. E. Newman
Physics Dept.
Univ. of Alaska
Fairbanks AK 99775
ffden@uaf.edu

Abstract

As power system loading increases, larger blackouts due to cascading outages become more likely. We investigate a critical loading at which the average size of blackouts increases sharply to examine whether the probability distribution of blackout sizes shows the power tails observed in real blackout data. Three different models are used, including two simulations of cascading outages in electric power transmission systems. We also derive and use a new, analytically solvable model of probabilistic cascading failure which represents the progressive system weakening as the cascade proceeds.

1. Introduction

Analyses [5, 8] of 15 years of North American blackout data [1] show a probability distribution of blackout size which has heavy tails and evidence of power law dependence in these tails [5, 8]. These analyses show that large blackouts are much more likely than might be expected from, say, a Gaussian distribution of blackout size in which the tails decay exponentially. The power tails of probability distributions of blackout size merit attention because of the enormous cost to society of large blackouts.

In complex systems, power tails in probability distributions are associated with systems at criticality. Other indicators of criticality are changes in gradient or a discontinuity in some measured quantity. One purpose of this paper is to examine the occurrence of power tails and criticality as power system loading is varied. We examine expected blackout size and pdfs as loading is varied in three different models. The first model is a simple analytic model of cascading failure and the second and third models are simulations of cascading outages in electric power transmission systems. In any power system, at zero loading there are no blackouts and at any absurdly large loading there is always a blackout. We examine the nature of the transition between these two extremes.

2. CASCADE model

We want to capture some general features of probabilistic cascading failure in a new model simple enough to allow exact analysis. The general features are:

1. Multiple components, each of which has a random initial loading.
2. When a component overloads, it fails and transfers some load to the other components.

Property 2 can cause cascading failure: an overload additionally loads other components and some of these other components may also overload, leading to a possible cascade of overloads. The extent of the cascade depends on the random initial component loadings. The components which are not (yet) overloaded become progressively more loaded as the cascade proceeds. Thus CASCADE models the weakening of the system as the cascade proceeds.

2.1. Description of model

The CASCADE model has n identical transmission lines with initial loadings (power flows) which are random. For each line the minimum loading is L^{min} and the maximum loading is 1. For j=1,2,...,n, line j has initial loading L_j which is a random variable uniformly distributed on $[L^{min},1]$. The average loading $L=(L^{min}+1)/2$. Also $L^{min}=2L-1$. $L_1,L_2,\cdots,L_n$ are independent.

Lines are outaged when their loading exceeds 1. When a line is outaged, a fixed amount of load Δ is transferred to each of the lines. Thus Δ is the amount of load increase on any line when another line outages. Let p be the probability that L_1 lies in an interval of length Δ contained in $[L^{min},1]$:

$$p=\frac{\Delta}{1-L^{min}}=\frac{\Delta}{2-2L} \qquad (1)$$

It is convenient to assume that the values of Δ are quantized so that $q=1/p=(1-L^{min})/\Delta$ is an integer. Then $[L^{min},1]$ can be partitioned into q intervals of length Δ.

To start the cascade, we assume an initial disturbance which loads each line by an additional amount Δ. Other lines may then outage depending on their loadings L_j and the outage of any of these lines will distribute an additional loading Δ that can cause further outages in a cascade.

The model parameters are summarized in Table 1. All the model parameters can be specified in terms of the average line loading L, the amount of load Δ distributed to each line upon an overload, and the number of lines n.

Table 1. CASCADE parameters

	description	comment
n	number of lines	
L	average line loading	
1	max line loading	
L^{min}	min line loading	$L^{min} = 2L - 1$
Δ	load increase at each line when outage	
p	probability L_1 in interval of length Δ	$p = \Delta/(2 - 2L)$
q	the integer $1/p$	$q\Delta = 1 - L^{min}$

2.2. Discussion of model

It is plausible that the general features of cascading failure captured in CASCADE can be present in cascading failure of power system transmission lines. However, CASCADE is much too simple to represent with realism most of the detailed and probably significant aspects of a power system. Obvious deficiencies of CASCADE include the transfer of loading upon overload without regard to network structure, an artificial uniformity in the transmission lines and their interactions, and no representation of generation changes or failure. Analysis of CASCADE can only suggest general qualitative behavior that may be present in power system cascading failures.

We discuss the parameter Δ. In a power system, suppose that a transmission line has maximum loading 1 and it overloads by a small amount so that the loading just before outage is approximately 1. Then, assuming a DC load flow model, the outage causes the other line flows to change according to line outage distribution factors [12]. The parameter Δ in CASCADE corresponds to line outage distribution factors averaged over all lines and all outaged lines. In practice, the line outage distribution factors vary considerably according to the lines considered. Only a subset of lines may have loading significantly increased or decreased by an outage.

If Δ is very roughly estimated by averaging line outage distribution factors, then it depends on the average amount of parallel paths in the network. In the special case of a network of all parallel lines, the amount of load transferred to other lines is $1/(\text{number of intact lines} - 1) \approx 1/n$, at least for the first few outages. In the case of the 179 bus model of the WSCC system with number of lines $n = 204$, the average line outage distribution factor is $0.0026 \approx 1/(2n)$. More highly meshed networks such as those in the Midwestern United States would tend to have smaller average line outage distribution factors.

In some cascading failures, power is redispatched so that an overload on a line is relieved. This also transfers power to other lines, but much less power is transferred than when the line outages. This process corresponds to a smaller value of Δ. There are also many other ways in which a disturbance can outage lines, including interactions via dynamics and via the protection system.

The overload of a line by redistribution of the power flow when another line outages depends both on the line loading and the line outage distribution factor. The CASCADE model has a fixed Δ corresponding to the line outage distribution factor but represents random variation in the line loadings.

2.3. Distribution of blackout size

Measure blackout size by S, the number of lines outaged. S is a discrete random variable on $0, 1, 2, ..., n$. The distribution of S is derived in appendix A and is given by the following formulas:

If $np \leq 1$ then

$$P[S = r] = \frac{1}{r+1}\binom{n}{r}((r+1)p)^r(1-(r+1)p)^{n-r} \tag{2}$$

If $np \geq 1$, then $q = 1/p \leq n$ and

$$P[S = r] = \begin{cases} \text{equation (2)} & ; r \leq q-1 \\ 0 & ; q \leq r \leq n-1 \\ 1 - \sum_{s=0}^{n-1} P[S = s] & ; r = n \end{cases} \tag{3}$$

Note that (2) gives $P[S = q-1] = 0$ and that (2) and (3) agree for $np = 1$.

Consul [9] introduced the following quasibinomial distribution to model an urn problem in which the player makes strategic decisions:

$$P[X = r] = \binom{n}{r} p(p + r\phi)^{r-1}(1 - p - r\phi)^{n-r} \tag{4}$$

for $r = 0, 1, ..., n$ and $p + n\phi \leq 1$. For the special case $\phi = p$ and $(n+1)p \leq 1$, we have $X = S$ and that S has the quasibinomial distribution. Consul [9] has derived the mean of distribution (4) and by setting $\phi = p$ in Consul's formula, we obtain

$$ES = np \sum_{r=0}^{n-1} \frac{(n-1)!}{(n-r-1)!} p^r \qquad , np \leq 1 \qquad (5)$$

2.4. Results

The distribution of blackout size S defined by (2), (3) depends on p and n. For the first series of results we use 100 lines ($n = 100$). The mean blackout size ES as a function of p is shown in Figure 1. There is a change in slope near $p = 0.01 = 1/100$ and, for larger p, the mean blackout size saturates at 100 lines.

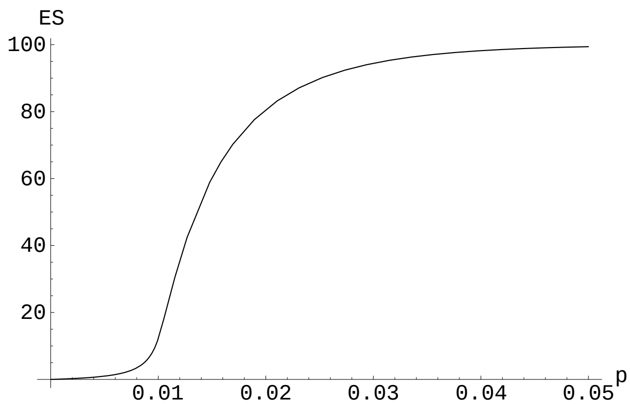

Figure 1. Mean blackout size ES versus probability p for $n = 100$.

Choose $\Delta = 0.005 = 1/(2n)$. Then the mean blackout size ES as a function of average loading L is shown by the solid line in Figure 2. For a fixed Δ, Figure 2 is obtained from Figure 1 by changing the horizontal axis quantity according to $L = 1 - \Delta/(2p)$. For $\Delta = 0.005$, the change in slope in Figure 2 corresponds to p near 0.01 and occurs near loading $L = 1 - 0.005/0.02 = 0.75$.

In the CASCADE model we can roughly approximate the mean power served as proportional to the average line loading and to the average number of intact lines:

$$\text{mean power served} \propto L(n - ES) \qquad (6)$$

Mean power served is plotted in Figure 2. The maximum mean power served occurs at the critical loading as a consequence of the sharp rise in ES becoming dominant in (6).

Figure 3 shows the distribution of S for $p = 0.005$ on a log-log plot. The distribution of S falls off for larger blackouts in a more exponential fashion and the probability of most or all of the lines blacking out is negligible.

Figure 4 shows the distribution of S when p is increased to the critical value of $p = 1/n = 0.01$. There is a heavy tail

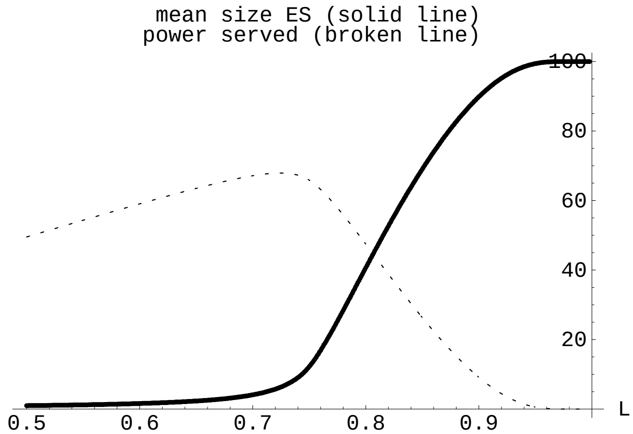

Figure 2. Mean blackout size ES and mean power served versus loading L. Power served has arbitrary units and $n = 100$.

in the distribution in which there is non-negligible probability of most or all of the lines blacking out. The distribution of S over an initial range of say, 0 to 25, is close to, but not exactly a power law. The region of behavior close to a power law is maximized for $p \approx 1/n = 0.01$.

Figure 5 shows the distribution of S when p is further increased to $p = 0.015$. The probability of the entire network blacking out is 0.60. There is also significant probability of short cascades and the distribution of these short cascades falls off in a more exponential fashion.

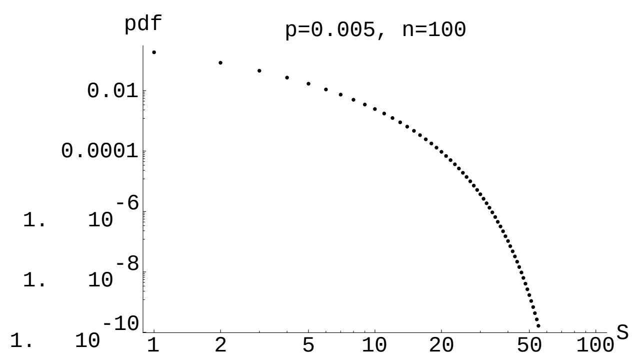

Figure 3. PDF of blackout size S. (P[S=0]=0.61 is not plotted.)

Now we briefly examine the scaling of the critical change in slope in Figure 1 with the number of lines n. It is useful to express the mean blackout size as the mean fraction of lines failed and to examine the mean blackout size as a function of the scaled probability np. Figure 6 shows the slope change for $n = 20, 100, 500$. The change in slope

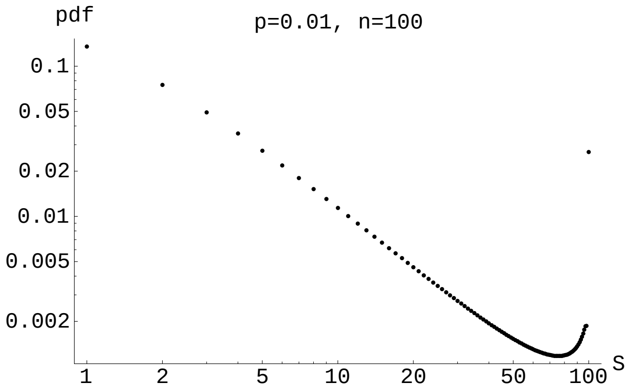

Figure 4. PDF of blackout size S. (P[S=0]=0.37 is not plotted.)

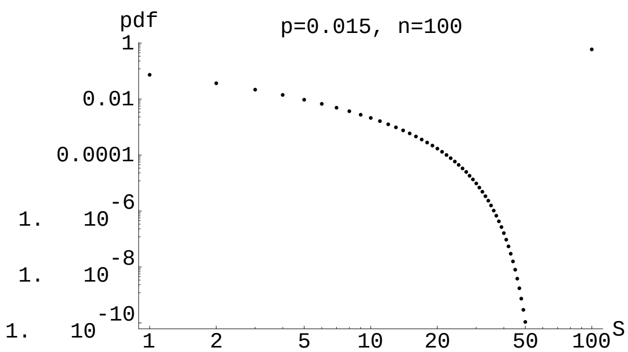

Figure 5. PDF of blackout size S. (P[S=0]=0.22 not plotted; note P[S=100]=0.60)

in Figure 6 occurs at $np = 1$ and becomes sharper as n increases. The slopes of the curves in Figure 6 peak at $np = 1$. These features of Figure 6 suggest a type 2 phase transition at $np = 1$. There is also a change in regime from formula (2) to formula (3) when $np = 1$.

We can analytically approximate the pdf of blackout size. Using Stirling's formula $m! \approx \sqrt{2\pi m}\,(m/e)^m$ to approximate the factor $n!/((r+1)!(n-r)!)$ in (2),

$$P[S=r] \approx \frac{e}{\sqrt{2\pi}}\sqrt{\frac{n}{n-r}}\frac{(np)^r}{(r+1)^{3/2}}\left(1+\frac{r-(r+1)np}{n-r}\right)^{n-r} \quad (7)$$

and, for large enough $n-r$, using $(1+y/(n-r))^{(n-r)} \approx e^y$ and $\sqrt{1-r/n} \approx 1$, we get

$$P[S=r] \approx \frac{(np)^r e^{(1-np)(r+1)}}{\sqrt{2\pi}\,(r+1)^{3/2}} \quad (8)$$

In approximation (8), the distribution of S depends only on

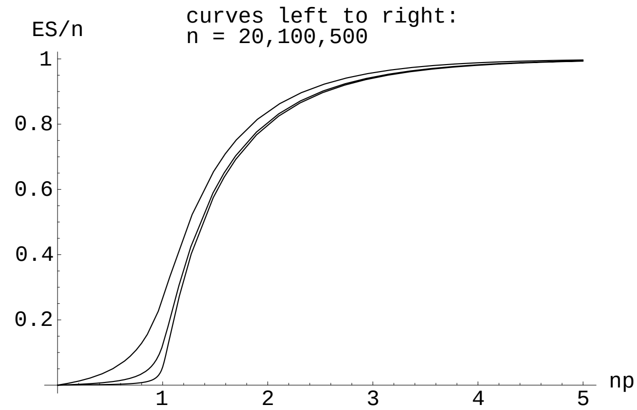

Figure 6. Fractional mean blackout size ES/n versus scaled probability np.

np. Moreover, if $np = 1$, then

$$P[S=r] \approx \frac{1}{\sqrt{2\pi}\,(r+1)^{3/2}} \quad (9)$$

and (9) predicts that the slope in Figure 4 is ≈ -1.5. The actual slope in Figure 4 varies between -1.0 and -1.3 for $2 \leq S \leq 45$ and is ≈ -1.3 for $6 \leq S \leq 28$. For np not close to 1, the expression $(np\,e^{(1-np)})^r$ in (8) will cause the distribution to decrease more exponentially for $r << n$.

The increased prevalence of large blackouts near critical loading can be attributed to the progressive loading and weakening of the network as lines outage. If one removes the progressive loading so that there is no increase of load when lines outage ($\Delta = 0$), but retain the initial disturbance of Δ, then the distribution of blackout sizes becomes binomial:

$$P[S=r] = \binom{n}{r} p^r (1-p)^{n-r} \quad (10)$$

3. Hidden Failure Model

When a transmission line trips, there is a small but significant probability that lines connected to either end of the tripped transmission line may incorrectly trip due to relay misoperation. These further line trippings are called hidden failures because they do not become apparent until the first line tripping "exposes" the adjacent lines to the possibility of relay misoperation. Recent NERC reports [1] show that hidden failures in protection systems have played a significant role in cascading disturbances. In this section, we summarize the hidden failure model presented in [8] and show simulation results about how the blackouts depend on system loading.

The hidden failure model uses the DC load flow approximation, in which the linearized, lossless power system is equivalent to a resistive circuit with current sources. In particular, transmission lines may be regarded as resistors and generation and load may be regarded as current sources and sinks. The probability of an exposed line tripping incorrectly is modeled as a increasing function of the line flow seen by the line relay. The probability is low below the line limit, and increases linearly to 1 when the line flow is 1.4 times the line limit.

The simulation begins by randomly choosing an initial line trip. This action exposes all lines connected to the ends of the initial line and also may overload lines. If one line flow exceeds its preset limit then the line is tripped. Otherwise, a line protection hidden failure mechanism [2, 11] is applied to let the chosen exposed line trip. After each line trip, the line flows are recalculated and checked for violations in line limits. The process is repeated until the cascading event stops.

As a final step, an optimal distribution of generation and load is calculated. Linear programming is used to minimize the amount of load shed subject to the constraints of the generation and load lying within their upper and lower limits, the line flows not exceeding the maximum flow, and overall generation matching the overall load.

The above simulation is repeated over an ensemble of randomly selected transmission lines as the initiating fault location.

We discuss an improvement of the hidden failure model. Suppose that a line is exposed multiple times by trippings of multiple lines connected to it. One would expect that, if relay misoperation occurs, it will occur on the first exposure of the line and is unlikely to occur on the subsequent exposures. However, the previous version of the model in [8, 2, 11] allowed relay misoperation with equal probability on all the line exposures. The improved model reduces or zeros the probability of misoperation after the first exposure.

We simulate a WSCC equivalent system with 179 buses, 29 generators, 60 transformers, and 203 transmission lines. The initial load flow data is based on the December 12, 1994 conditions, from which the required DC load flow data is derived.

NERC reports [1] show that there are only about 150 events during the past 16 years in the WSCC region. A direct simulation of these rare events would require an unrealistically huge amount of computation. One way out of this quandary is to use importance sampling [3]. In importance sampling, rather than using the actual probabilities, the simulation uses altered probabilities so that the rare events occur more frequently. Associated with each distinct sample path, SP_i, a ratio of actual probability of the event p_i^{actual} divided by the altered probability $p_i^{simulate}$ is computed. We then form the estimated probability of SP_i as

$$\hat{\rho}_i = \frac{N_{occurring}}{N_{total}} \cdot \frac{p_i^{actual}}{p_i^{simulate}} \tag{11}$$

where $N_{occurring}$ is the number of times that SP_i occurred and N_{total} is the total number of samples. The mean value of $\hat{\rho}_i$ is unbiased [3]. The power loss P_i associated with each sample path is also recorded.

Figure 7 shows the expected power loss

$$EP = \sum P_i \, \hat{\rho}_i \tag{12}$$

as a function of loading level L. The change in slope occurs near loading $L = 0.75$.

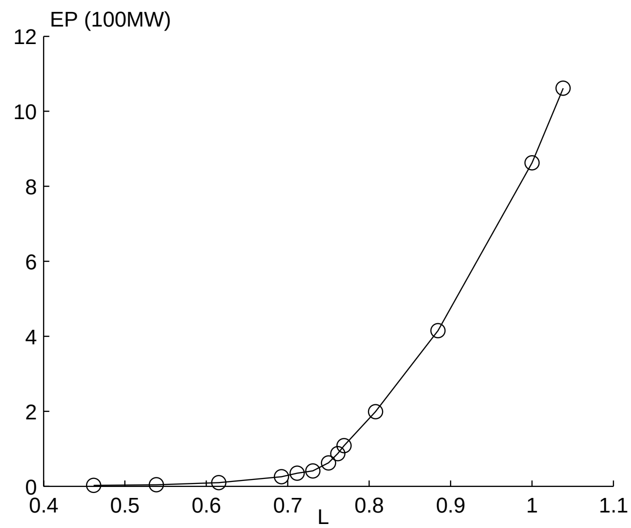

Figure 7. Variation of expected blackout size EP with loading L

To find out the probability distribution of blackout size P, binning of the data is used. Assume there are K sample points in bin j, and that each of the K points has the associated data pair $(P_i, \hat{\rho}_i)$. The representative $(\bar{P}_j, \bar{\hat{\rho}}_j)$ for bin j is defined as

$$\bar{P}_j = \frac{1}{K}\sum_{i=1}^{K} P_i \quad \text{and} \quad \bar{\hat{\rho}}_j = \frac{\sum_{i=1}^{K} P_i \hat{\rho}_i}{\bar{P}_j} \tag{13}$$

The variable binning used here is such that each bin starts with the minimum width and ends with at least a minimum number of samples.

Figures 8, 9, 10 show the pdf of blackout size P at the critical loading level 0.75, a higher level 0.85, and a lower level 0.62. The pdfs for loading levels 0.75 and 0.85 show some evidence of power tails. The 4 data points in Figure 9

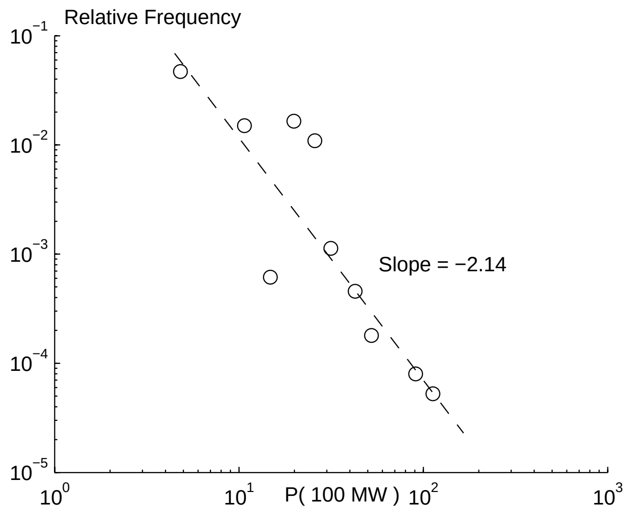

Figure 8. Distribution of blackout size P at loading $L = 0.75$

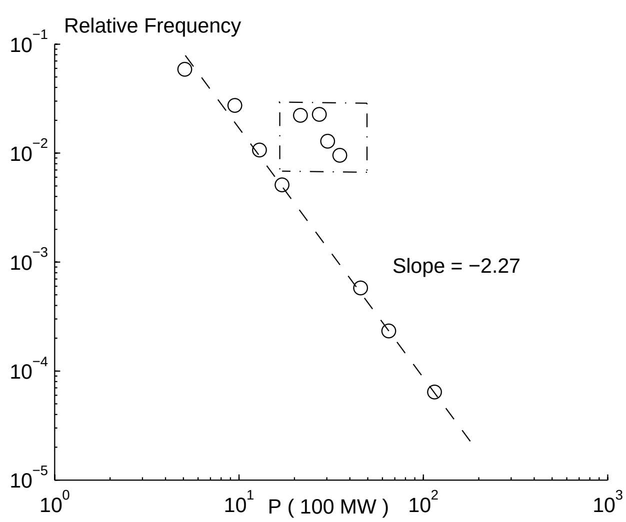

Figure 9. Distribution of blackout size P at loading $L = 0.85$

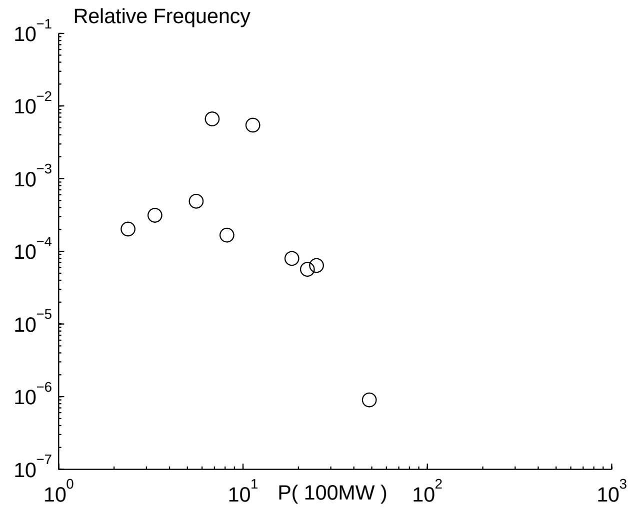

Figure 10. Distribution of blackout size P at loading $L = 0.62$

that lie well above the dotted line indicate a higher probability of medium size blackouts. This arises from artificial limitations on the further spread of blackouts of medium size, particularly the suppression of tripping in 45 negative impedance lines that represent highly equivalenced portions of network and in 60 lines that represent transformers (transformer failures are not modelled).

4. OPA model

The OPA model was developed to assess the possibility of self-organized criticality in series of electric power blackouts [10, 5, 7]. The self organization arises from the opposing forces of load growth and network upgrades in response to blackouts. In this paper we use a version of OPA with no load growth and a fixed network and it is this version which is summarized. For more detail see [10, 5, 7].

The OPA model represents transmission lines, loads and generators with the usual DC load flow assumptions. Starting from a solved base case, blackouts are initiated by a random line outage. Whenever a line is outaged, the generation and load is redispatched using standard linear programming methods. The cost function is weighted to ensure that load shedding is avoided where possible. If any lines were overloaded during the optimization, then these lines are outaged with probability p_1. The process of redispatch and testing for outages is iterated until there are no more outages. Thus OPA represents generic cascading outages which are consistent with basic network and operational constraints. A record is kept of the line overloads and outages and the load shed so that the blackout extent can be studied. $p_1 = 0$ ensures there are no line outages and only line overloads are considered whereas $p_1 = 1$ ensures that all overloaded lines outage.

We consider a fixed network with parameters chosen so that the system will be constrained by its transmission capacity as the load is increased. The network has 94 nodes, 12 generators and 82 loads arranged in a regular network with a tree-like form [6]. Most nodes have 3 incident transmission lines. A random fluctuation in loads is assumed up to a maximum of 20%. Blackout size is measured by the amount of load shed.

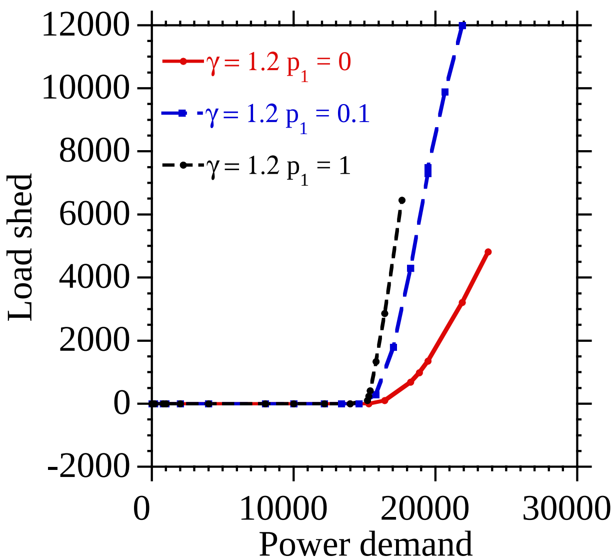

Figure 11. Mean blackout size versus loading.

Figure 11 shows mean blackout size as measured by the amount of load shed versus loading for three values of p_1. There is a critical loading $P = 15392$ at which the mean blackout size increases.

Figure 12 shows pdfs of blackout size as loading increases through the critical loading for $p_1 = 1$. The pdfs are shifted vertically so that their form may be seen.

At load $P = 15210$ (below the critical loading) the number of blackouts is small. The load fluctuations cause lines to overload and outage and hence some load shed. It common for a single line to outage so that only one load node is blacked out. This causes the pdf at lower blackout sizes to have a series of peaks associated with values of load at a single node.

At the critical loading $P = 15392$ there is some indication that a power tail develops with a decay index of about -1.5. The fall off after 0.08 is a network size effect. Above the critical loading the pdf is more Gaussian and is localized at a high value of the load shed.

The OPA model contains multiple critical points associ-

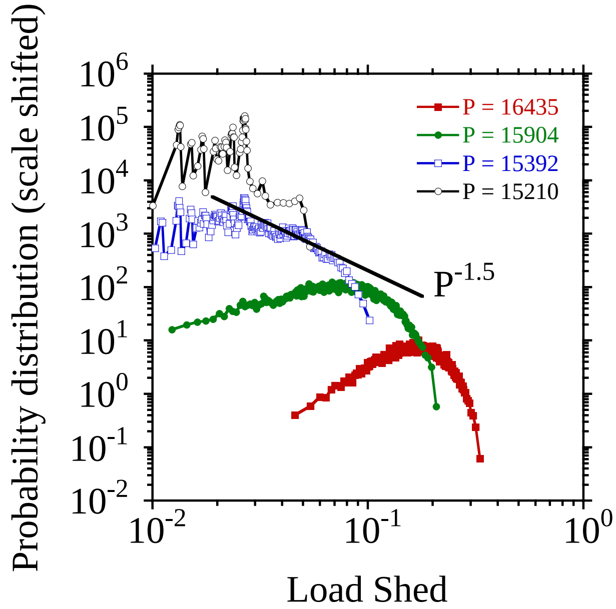

Figure 12. Distributions of blackout size.

ated with limits on both transmission and generation. In [7], we choose parameters so that the generation critical loading is reached first and scan through the critical loading by fixing the load and increasing the load fluctuations from zero to 98%. The results again show a power tail at the critical loading and a more exponential decay below and above the critical loading [7].

5. Discussion and Conclusions

We have examined expected blackout size and blackout size pdfs as load is increased in three different models: CASCADE, a hidden failure model, and the OPA model. All three models show a sharp increase in slope of the expected blackout size at a critical loading.

All three models show some evidence of power tails in the pdf at this critical loading, but there remain some differences and uncertainties in this result. In particular,

(1) CASCADE shows approximate power law behavior over a substantial range of blackout sizes near the critical loading. The CASCADE model is analytic so that the results are exact. CASCADE may represent processes occurring in cascading failure in power system but CASCADE is too simple to represent some presumably significant power system features.

(2) The hidden failure model shows power tails at and above the critical loading, except for some medium size blackouts. Below the critical loading the form of the pdf is not clear. This model represents hidden failures in the

protection system well and models power system cascading outages and overloads using the DC load flow approximation and LP redispatch. The results are obtained on a 179 bus equivalenced WSCC system.

(3) The OPA model shows some evidence of a power law region at critical loading and a more Gaussian form at higher or lower loadings. This model represents generic cascading power system outages and overloads using the DC load flow approximation and LP redispatch. The results are obtained on an artificial symmetric power system network of 96 nodes.

Since the three models are quite different and even the two simulation models are very approximate power system models, one cannot expect detailed agreement between the models or, for that matter, between the models and a real power system. (For example, [7] shows that the critical behavior of the OPA model is complicated and certainly cannot be reproduced in detail by CASCADE.) However, the broad agreement between the models is consistent with and supportive of the hypothesis that power tails in the pdf appear at a critical loading at which mean blackout size increases sharply. Moreover, it is possible that general features of cascading outages in power systems are captured by all three models; and in this case, the strengthened hypothesis is progress towards a global analysis and understanding of cascading failures in power systems. Further work testing the hypothesis to gain sharper conclusions is indicated.

Indeed, the hypothesis, if fully established, would have significant consequences for power system operation. For then the NERC blackout data [1, 5, 8] suggests that the North American power system has been operated near criticality. Moreover, it is then plausible that the power tails and the consequent risk of large blackouts could be substantially reduced by lowering power system loading to obtain an exponential tail for large blackouts. It would be better to analyze this tradeoff between catastrophic blackout risk and loading instead of just waiting for the effects to manifest themselves in the North American power system!

Why would power systems be operated near a critical loading? One possible answer is that overall forces, including the system engineering and operational policies, organize the system towards criticality as proposed in [4, 5, 10, 6, 7].

A notable outcome of this paper is the CASCADE model and the derivation of formulas for its pdf. This pdf exhibits heavy tails near critical loading and more exponential tails far from critical loading (high loading also yields a significant chance of total failure). This is a new model of probabilistic cascading failure that is of general interest in studying the distribution of sizes of failures of large interconnected systems in which the successive failure of loaded components progressively weakens the system.

6. Acknowledgements

I. Dobson, J.S. Thorp, J. Chen, and B.A. Carreras gratefully acknowledge coordination of this work by the Consortium for Electric Reliability Technology Solutions and funding in part by the Assistant Secretary for Energy Efficiency and Renewable Energy, Office of Power Technologies, Transmission Reliability Program of the U.S. Department of Energy under contract 9908935 and Interagency Agreement DE-A1099EE35075 with the National Science Foundation. I. Dobson and D.E. Newman gratefully acknowledge support in part from National Science Foundation grants ECS-0085711 and ECS-0085647. Part of this research has been carried out at Oak Ridge National Laboratory, managed by UT-Battelle, LLC, for the U.S. Department of Energy under contract number DE-AC05-00OR22725. I. Dobson thanks H-D. Chiang and the School of ECE at Cornell University for their generous hospitality during a sabbatical leave.

References

[1] Information on electric systems disturbances in North America can be downloaded from the NERC website at http://www.nerc.com/dawg/database.html

[2] K. Bae, J.S. Thorp, A stochastic study of hidden failures in power system protection, Decision Support Systems, vol. 24, pp. 259-268, 1999.

[3] J.A. Bucklew, Large deviation techniques in decision, simulation, and estimation, Wiley 1990.

[4] B.A. Carreras, D.E. Newman, I. Dobson, A.B. Poole, Initial evidence for self-organized criticality in electric power system blackouts, 33rd Hawaii International Conference on System Sciences, Maui, Hawaii, January 2000.

[5] B.A. Carreras, D.E. Newman, I. Dobson, A.B. Poole, Evidence for self-organized criticality in electric power system blackouts, 34th Hawaii International Conference on System Sciences, Maui, Hawaii, January 2001.

[6] B.A. Carreras, V.E. Lynch, M. L. Sachtjen, I. Dobson, D.E. Newman, Modeling blackout dynamics in power transmission networks with simple structure, 34th Hawaii International Conference on System Sciences, Maui, Hawaii, January 2001.

[7] B.A. Carreras, V.E. Lynch, I. Dobson, D.E. Newman, Dynamics, criticality and self-organization in a model for blackouts in power transmission systems, 35th Hawaii International Conference on System Sciences, Hawaii, January 2002.

[8] J. Chen, J.S. Thorp, M. Parashar, Analysis of electric power disturbance data, 34th Hawaii International Conference on System Sciences, Maui, Hawaii, January 2001.

[9] P.C. Consul, A simple urn model dependent upon predetermined strategy, Sankhyā: The Indian Journal of Statistics, Series B, vol. 36, Pt. 4, 1974, pp. 391-399.

[10] I. Dobson, B.A. Carreras, V. Lynch, D.E. Newman, An initial model for complex dynamics in electric power system blackouts, 34th Hawaii International Conference on System Sciences, Maui, Hawaii, January 2001.

[11] J.S. Thorp, A.G. Phadke, et al., Anatomy of power system disturbances: Importance sampling, Power System Computation Conference, Dresden, Aug. 1996.

[12] A.J. Wood, B.F. Wollenberg, Power system generation, operation and control, Wiley 1984.

A. Derivation of CASCADE distribution

It is convenient to to work in terms of line margins $M_1, M_2, M_3, \cdots, M_n$ where $M_j = 1 - L_j$. Then $M_1, M_2, M_3, \cdots, M_n$ are independent random variables uniform on $[0, 1 - L^{min}]$. Recall that the integer $q = (1 - L^{min})/\Delta = 1/p$.

We suppose that $r \le q - 1$ and examine the event $[S = r]$, which is a cascade of exactly r lines. Suppose we renumber the lines so that the r lines outaged in the order $1, 2, ..., r$. The initial disturbance increased the loading on line 1 by Δ. Since line 1 outaged, its margin M_1 must have been less than Δ. The outage of line 1 caused an additional increase of loading Δ on all the lines. Since line 2 outaged, its margin M_2 must have been less than 2Δ. Similarly, for $j \le r$, since line j outaged, its margin M_j must have been less than $j\Delta$. After line r outages, the remaining intact lines all have had their loadings increased by $(r+1)\Delta$. ($(r+1)\Delta$ comprises the initial disturbance Δ and Δ for each of the r lines outaged.) Since none of the remaining intact lines outaged, their margins must all exceed or equal $(r + 1)\Delta$. To summarize:

$$M_1 < \Delta, M_2 < 2\Delta, \cdots, M_r < r\Delta,$$
$$M_k \ge (r + 1)\Delta \qquad \text{for } r + 1 \le k \le n.$$

The same argument without renumbering the lines and accounting for the possible permutations of lines yields

$$[S = r] = \bigcup_{\pi \in S_n} [M_{\pi(1)} < \Delta, M_{\pi(2)} < 2\Delta, \cdots, M_{\pi(r)} < r\Delta, M_{\pi(r+1)} \ge (r + 1)\Delta, \cdots, M_{\pi(n)} \ge (r + 1)\Delta] \quad (14)$$

where the union runs over all permutations π of $1, 2, \cdots, n$ in the symmetric group S_n. The union in (14) is not a disjoint union.

We consider the case $r > q - 1$. If the cascade extends to a size $r > q - 1$, then the total increase in load on the remaining intact lines is $(r+1)\Delta > q\Delta = 1 - L^{min}$. Since $1 - L^{min}$ is the maximum line margin, all the remaining intact lines must outage, and so $S = n$ and $P[S = r] = 0$ for $q - 1 < r < n$.

In the case $r = q - 1$, (14) applies but, since $(r + 1)\Delta = q\Delta = 1 - L^{min}$, the event $[M_{\pi(n)} \ge (r + 1)\Delta]$ becomes the probability zero event $[M_{\pi(n)} = 1 - L^{min}]$ and hence $P[S = q - 1] = 0$.

Now we assume $r < q - 1$ for the rest of this appendix. Define intervals $I_1, I_2, \cdots, I_q$ so that

$$I_j = [(j - 1)\Delta, j\Delta) \quad ; 1 \le j \le q \quad (15)$$

Then
$$[M_{\pi(\ell)} < \ell\Delta] = \bigcup_{a_\ell \in \{1,2,...,\ell\}} [M_{\pi(\ell)} \in I_{a_\ell}]$$
$$[M_{\pi(\ell)} \ge (r + 1)\Delta] = \bigcup_{a_\ell \in \{r+2,...,q\}} [M_{\pi(\ell)} \in I_{a_\ell}]$$

and (14) can be written as

$$[S = r] = \bigcup_{\pi \in S_n} \bigcup_{(a_1,a_2,...,a_n) \in B} [M_{\pi(1)} \in I_{a_1}, M_{\pi(2)} \in I_{a_2}, \cdots, M_{\pi(n)} \in I_{a_n}] \quad (16)$$

where $B = \{(a_1, a_2, ..., a_n) \mid a_1 \in \{1\}, a_2 \in \{1, 2\}, ..., a_r \in \{1, 2, ..., r\}, a_{r+1} \in \{r + 2, ..., q\}, ..., a_n \in \{r + 2, ..., q\}\}$

In (16) it is equivalent to permute the intervals I_{a_i} instead of permuting the margins M_i:

$$[S = r] = \bigcup_{\pi \in S_n} \bigcup_{(a_1,a_2,...,a_n) \in B} [M_1 \in I_{a_{\pi(1)}}, M_2 \in I_{a_{\pi(2)}}, \cdots, M_n \in I_{a_{\pi(n)}}] \quad (17)$$

and (17) may be rewritten as

$$[S = r] = \bigcup_{(a_1,a_2,...,a_n) \in B_\pi} [M_1 \in I_{a_1}, M_2 \in I_{a_2}, \cdots, M_n \in I_{a_n}] \quad (18)$$

where B_π is the set of permuted elements of B:

$$B_\pi = \bigcup_{\pi \in S_n} \{(a_{\pi(1)}, a_{\pi(2)}, ..., a_{\pi(n)}) \mid a_1 \in \{1\}, a_2 \in \{1, 2\}, ..., a_r \in \{1, 2, ..., r\}, a_{r+1} \in \{r + 2, ..., q\}, ..., a_n \in \{r + 2, ..., q\}\} \quad (19)$$

For each i with $1 \le i \le n$, the event $[M_i \in I_{a_i}]$ has probability p. Since $M_1, M_2, \cdots, M_n$ are independent, the event $[M_1 \in I_{a_1}, M_2 \in I_{a_2}, \cdots, M_n \in I_{a_n}]$ has probability p^n. Equation (18) expresses $[S = r]$ as a disjoint union of events $[M_1 \in I_{a_1}, M_2 \in I_{a_2}, \cdots, M_n \in I_{a_n}]$. Therefore, writing $|B_\pi|$ for the number of elements of B_π,

$$P[S = r] = |B_\pi|\, p^n \quad (20)$$

and the computation of $P[S = r]$ reduces to counting the number of elements of B_π.

$$\begin{aligned} \text{Define} \quad A_r = & \bigcup_{\pi \in S_r} \{(a_{\pi(1)}, a_{\pi(2)}, ..., a_{\pi(r)}) \mid \\ & a_1 \in \{1\}, a_2 \in \{1,2\}, ..., a_r \in \{1,2,...,r\}\} \quad (21) \\ A'_r = & \bigcup_{\pi \in S_{n-r}} \{(a_{\pi(1)}, a_{\pi(2)}, ..., a_{\pi(n-r)}) \mid \\ & a_1 \in \{r+2, ..., q\}, ..., a_{n-r} \in \{r+2, ..., q\}] \end{aligned}$$

Each element of B_π can be uniquely specified by first choosing which $n-r$ of $\{a_1, a_2, ..., a_n\}$ are in $\{r+2, ..., q\}$, or, equivalently, which r of $\{a_1, a_2, ..., a_n\}$ are less than $r+1$, and then making a choice of one element of A_r, and then making a choice of one element of A'_r. Therefore

$$|B_\pi| = \binom{n}{n-r} |A_r||A'_r| = \binom{n}{r} |A_r||A'_r| \quad (22)$$

It is straightforward that $|A'_r| = (q-(r+1))^{n-r}$ and Lemma 1 below yields $|A_r| = (r+1)^{r-1}$. Hence

$$|B_\pi| = \binom{n}{r} (r+1)^{r-1} (q-(r+1))^{n-r} \quad (23)$$

It follows from (20), (23) and $pq = 1$ that

$$P[S = r] = \frac{1}{r+1} \binom{n}{r} ((r+1)p)^r (1-(r+1)p)^{n-r} \quad (24)$$

Lemma 1 *Define the set* A_r *by* (21). *Then*

$$|A_r| = (r+1)^{r-1} \quad (25)$$

Proof: Define

$$\begin{aligned} \Sigma_{r+1} = & \{(a_1, a_2, ..., a_r) \mid \\ & a_i \in \{1, 2, ..., r+1\}, \ i = 1, 2, ..., r\} \quad (26) \end{aligned}$$

Then $A_r \subset \Sigma_{r+1}$ and $|\Sigma_{r+1}| = (r+1)^r$.

Define the permutation σ_1 on $\{1, 2, ..., r+1\}$ by

$$\sigma_1(a) = \begin{cases} a+1 & ; 1 \le a \le r \\ 1 & ; a = r+1 \end{cases} \quad (27)$$

Define $\sigma : \Sigma_{r+1} \to \Sigma_{r+1}$ by

$$\sigma((a_1, a_2, ..., a_r)) = (\sigma_1(a_1), \sigma_1(a_2), ..., \sigma_1(a_r)) \quad (28)$$

σ^{r+1} is the identity and $\{1, \sigma, \sigma^2, ..., \sigma^r\}$ is a cyclic group acting on Σ_{r+1}.

Consider the following union of subsets of Σ_{r+1}:

$$A_r \cup \sigma(A_r) \cup \sigma^2(A_r) \cup \cdots \cup \sigma^r(A_r) \quad (29)$$

To prove the Lemma it is sufficient to show that (29) is a partition of Σ_{r+1} into $r+1$ sets of equal size. For then $(r+1)|A_r| = |\Sigma_{r+1}| = (r+1)^r$.

The equal size of $A_r, \sigma(A_r), \sigma^2(A_r), \cdots, \sigma^r(A_r)$ follows from σ being a bijection. To prove that (29) is a partition, we need $A_r, \sigma(A_r), \sigma^2(A_r), \cdots, \sigma^r(A_r)$ to be disjoint and that (29) is equal to Σ_{r+1}.

Let k satisfy $1 \le k \le r$.

$$\begin{aligned} \sigma^k(A_r) = & \bigcup_{\pi \in S_r} \{(a_{\pi(1)}, a_{\pi(2)}, ..., a_{\pi(r)}) \mid \\ & a_1 \in \{k+1\}, \\ & a_2 \in \{k+1, k+2\}, \cdots, \\ & a_{r+1-k} \in \{k+1, ..., r+1\}, \\ & a_{r+2-k} \in \{k+1, ..., r+1, 1\}, \\ & a_{r+3-k} \in \{k+1, ..., r+1, 1, 2\}, \cdots, \\ & a_r \in \{k+1, ..., r+1, 1, 2, ..., k-1\}\} (30) \end{aligned}$$

By inspection of (21) and (30), each element of A_r has at least k entries from $\{1, 2, ..., k\}$ and each element of $\sigma^k(A_r)$ has no more than $k-1$ entries from $\{1, 2, ..., k\}$. Therefore A_r and $\sigma^k(A_r)$ are disjoint for $1 \le k \le r$. Then $A_r, \sigma(A_r), \sigma^2(A_r), \cdots, \sigma^r(A_r)$ are disjoint, for if not, then there are m, ℓ with $0 \le m < \ell \le r$ and $1 \le \ell - m \le r$ and there is a $b \in \sigma^m(A_r) \cap \sigma^\ell(A_r)$ and $\sigma^{-m}(b) \in A_r \cap \sigma^{\ell-m}(A_r)$, which is a contradiction.

To show that the subset (29) of Σ_{r+1} is equal to Σ_{r+1}, we choose any $b = (b_1, b_2, ..., b_r) \in \Sigma_{r+1}$ and show that b is in (29). Define $|b| = |(b_1, b_2, ..., b_r)| = b_1 + b_2 + ... + b_r$. Choose k which minimizes $|\sigma^k(b)|$ and write $c = (c_1, c_2, ..., c_r) = \sigma^k(b)$.

We now show that $c \in A_r$. Since A_r contains all permutations of its elements, we can reorder $(c_1, c_2, ..., c_r)$ without loss of generality so that $c_1 \le c_2 \le ... \le c_r$. According to (21), $c_i \in \{1, 2, ..., i\}$, $i = 1, 2, ..., r$ implies $c \in A_r$. We prove $c_i \in \{1, 2, ..., i\}$, $i = 1, 2, ..., r$ by induction on i.

$c_1 \in \{1\}$, for if $c_1 > 1$, then $c_j \ge 2$ for $j = 1, 2, ..., r$ and $\sigma_1^{-1}(c_j) = c_j - 1$ for $j = 1, 2, ..., r$ and $|\sigma^{-1}(c)| = |c| - r < |c|$ which is a contradiction.

Now suppose that i satisfies $2 \le i \le r$ and that $c_\ell \in \{1, 2, ..., \ell\}$ for $\ell < i$. Then $\sigma_1^{-i}(c_j) = c_j + r + 1 - i$ for $j = 1, 2, ..., i-1$. Suppose that $c_i \notin \{1, 2, ..., i\}$. Then $c_j \ge i+1$ for $j = i, i+1, ..., r$ and $\sigma_1^{-i}(c_j) = c_j - i$ for $j = i, i+1, ..., r$. Now $|\sigma^{-i}(c)| = |c| + (i-1)(r+1-i) - (r+1-i)i = |c| - (r+1-i) < |c|$ which is a contradiction. Therefore $c_i \in \{1, 2, ..., i\}$.

Thus $c \in A_r$. It follows that $b = \sigma^{-k}(c) = \sigma^{r+1-k}(c) \in \sigma^{r+1-k}(A_r)$ is in (29).

6.3 Study on cascading dynamics in power transmission systems via a DC hidden failure model

J. Chen, J.S. Thorp

report November 2001

Study on Cascading Dynamics in Power Transmission Systems via a DC Hidden Failure Model

J. Chen
School of ECE, Cornell University
Ithaca NY 14853 USA
jchen@ece.cornell.edu

J.S. Thorp
School of ECE, Cornell University
Ithaca NY 14853 USA
thorp@ece.cornell.edu

Abstract

A DC model of power transmission systems has been developed to study the observed power tail of North American blackouts data [1,2]. We discuss in this paper a modified model with an improved hidden failure mechanism. Our focus here is to investigate the impacts of several system parameters on the global dynamics. The main parameters include system loading level, hidden failure probability, spinning reserve capacity and control strategy. The sensitivity of power-law behavior with respect to each of these parameters is discussed and illustrated using simulation results from the WSCC 179-bus equivalent system.

1. Introduction

Analysis of 16 years of North American blackout data [3] show a probability distribution of blackout size which has heavy tails and evidence of power law dependence in these tails [1]. The analysis show that large blackouts are much more likely than might be expected from, say, a Gaussian distribution of blackout size in which the tails decay exponentially. The power tails in blackout size probability distributions merit attention because of the enormous cost to society of large blackouts.

Recent NERC reports [3] show that protective relay malfunction significantly contributes to the cascading outages. A common scenario is that the relay has an undetected (hidden) defect that remains dormant until abnormal operating conditions are reached. In this paper, we developed a DC hidden failure model of power transmission systems to explore the characteristics of cascading events and the impacts of various model parameters on the system dynamics.

2. Hidden Failure Model

2.1. Description of Model

The hidden failure model uses the DC load flow approximation, in which the linearized, lossless power system is equivalent to a resistive circuit with current sources. In particular, transmission lines may be regarded as resistors and generation and load may be regarded as current sources and sinks at the nodes of the network. Line protection hidden failures are also incorporated to model protective relays. Each line has a different load dependent probability of incorrectly tripping. The probability of an exposed line tripping incorrectly is modeled as a increasing function of the line flow seen by the line relay. The probability is low below the line limit, and increases linearly to 1 when the line flow is 1.4 times the line limit.

The simulation begins by randomly choosing an initial line trip. This action exposes all lines connected to the ends of the initial line and also may overload lines. If one line flow exceeds its preset limit then the line is tripped. Otherwise, a line protection hidden failure mechanism [5] is applied to let the chosen exposed line trip. After each line trip, the line flow is recalculated and checked for violations in line limits. The process is repeated until the cascading event stops.

As a final step, an optimal distribution of generation and load is calculated. Linear programming is used to minimize the amount of load shed subject to the constraints of the generation and load lying within their upper and lower limits, the line flows not exceeding the maximum flow, and overall generation matching the overall load.

The above simulation is repeated over an ensemble of randomly selected transmission lines as the initiating fault location.

2.2. Importance Sampling Technique

We simulated a WSCC equivalent system with 179 buses, 29 generators, 60 transformers, and 203 transmission lines. The initial load flow data is based on the December 12, 1994 conditions, from which the required DC load flow data is derived.

NERC reports [3] show that there are only about 150 events during the past 16 years in the WSCC region. A direct simulation of these rare events would require an unrealistically huge amount of computation. One way out of this quandary is to use importance sampling [7]. In importance sampling, rather than using the actual probabilities, the simulation uses altered probabilities so that the rare events occur more frequently. Associated with each distinct sample path, SP_i, a ratio of actual probability of the event p_i^{actual} divided by the altered probability $p_i^{simulate}$ is computed. We then form the estimated probability of SP_i as

$$\hat{\rho}_i = \frac{N_{occurring}}{N_{total}} \cdot \frac{p_i^{actual}}{p_i^{simulate}} \tag{1}$$

where $N_{occurring}$ is the number of times that SP_i occurred and N_{total} is the total number of samples. The mean value of $\hat{\rho}_i$ is unbiased [7]. The power loss P_i associated with each sample path is also recorded.

2.3. Modified Hidden Failure Mechanism

We discuss an improvement of the previous hidden failure model. Suppose a line is exposed multiple times during a cascading event. One would expect that, if relay misoperation occurs, it would be more likely to occur on the first exposure than the subsequent exposures. However, the previous version of the model allowed relay misoperation with equal probability on all the line exposures. The improved model reduces or, for simplicity reduces the probability of misoperation after the first exposure to zero.

3. Parameter Sensitivity Study

3.1. Impact of Loading Level

In any power system, at zero loading there are no blackouts and at any absurdly large loading there is always a blackout. We examined the nature of the transition between these two extremes in this section.

Figure **??** shows the expected power loss

$$EP = \sum P_i \; \hat{\rho}_i \tag{2}$$

as a function of loading level L. The change in slope occurs near loading $L = 0.75$.

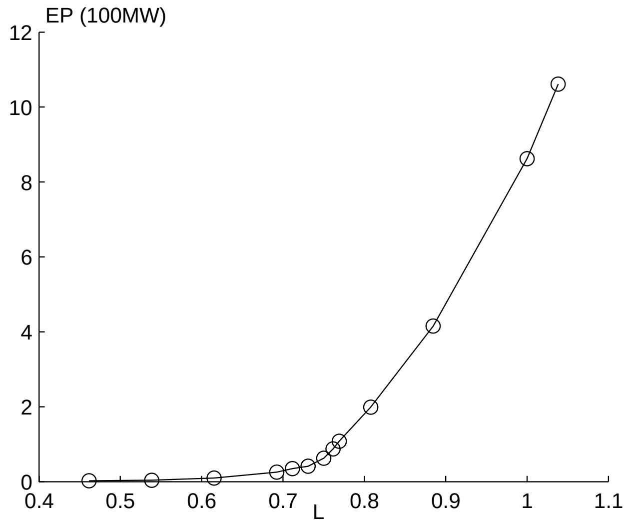

Figure 1. Variation of expected blackout size EP with loading L

To find out the probability distribution of blackout size P, binning of the data is used. Assume there are K sample points in bin j, and that each of the K points has the associated data pair $(P_i, \hat{\rho}_i)$. The representative $(\bar{P}_j, \bar{\hat{\rho}}_j)$ for bin j is defined as

$$\bar{P}_j = \frac{1}{K} \sum_{i=1}^{K} P_i \tag{3}$$

$$\bar{\hat{\rho}}_j = \frac{\sum_{i=1}^{K} P_i \hat{\rho}_i}{\bar{P}_j} \tag{4}$$

The variable binning is used here in such a way that each bin starts with the minimum scale and ends with at least a minimum number of samples.

Figures **??**, **??**, **??** show the pdf of blackout size P at critical loading level 0.75, a higher level 0.85, and a lower level 0.62. The pdfs of loading levels 0.75 and 0.85 show some evidence of power tails. The 4 data points in Figure **??** that lie well above the dotted line indicate a higher probability of medium size blackouts. This arises from artificial limitations on the further spread of blackouts of medium size, particularly the suppression of tripping in 45 negative impedence lines that represent highly equivalenced portions of network and in 60 lines that represent transformers(transformer failures are not modelled).

3.2. Impact of Spinning Reserve Capacity

Ample spinning reserve is a necessity to maintain system reliability in case of unit loss or other contingencies. In this section, we examined the impact of the capacity of available spinning reserve on the power tail of cascading events.

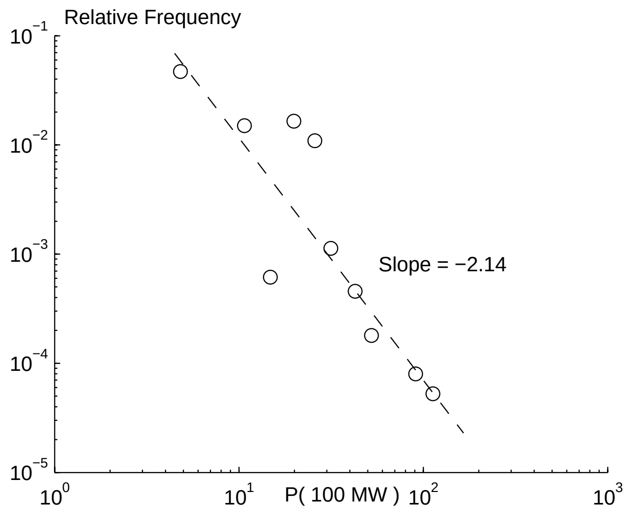

Figure 2. Distribution of blackout size P at loading $L = 0.75$

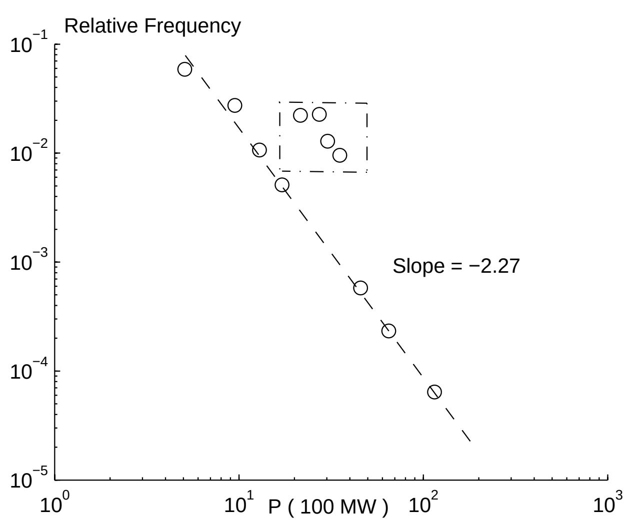

Figure 3. Distribution of blackout size P at loading $L = 0.85$

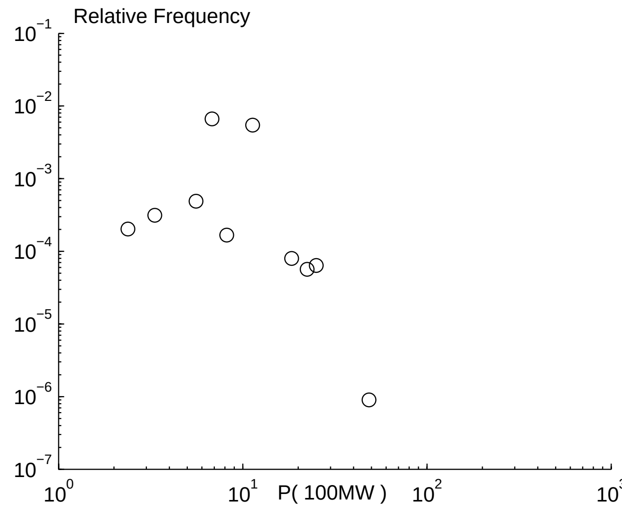

Figure 4. Distribution of blackout size P at loading $L = 0.62$

Usually certain rules set by regional reliability councils specify how the required reserve is allocated. Typically, reserve is needed to be a given percentage of forecasted peak load. Here, we assume that for each generator, the ratio of available spinning reserve, R, over its generation in base-load condition, P, is the same. For example, if the system reserve capacity is 10% of power demand, then for any generator i, its available reserve $R_i = 0.1 \times P_i$.

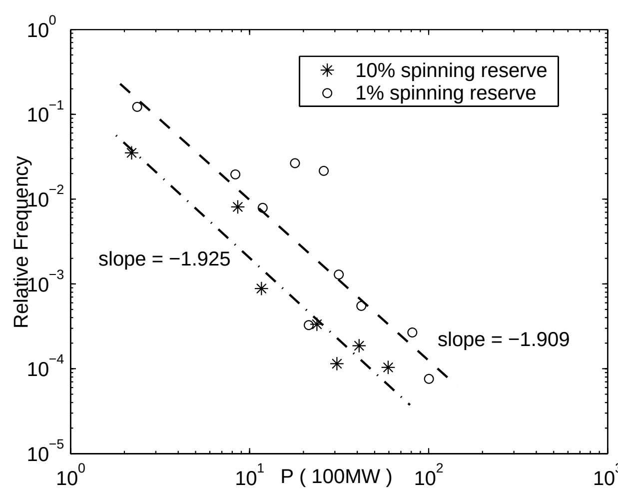

Figure 5. Distribution of blackout size P with reserve capacity of 1% and 10%

Figures **??**, **??** show the pdf of blackout size P with 1%, 10%, and 20% reserve capacity. The power tail is preserved with low reserve capacity, while changes to ”exponential

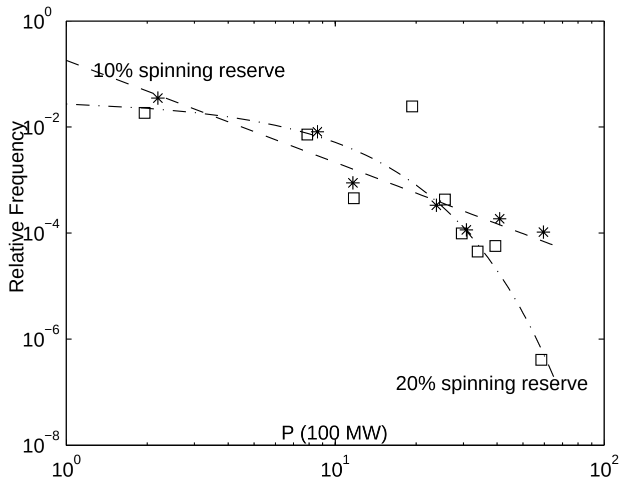

Figure 6. Distribution of blackout size P with reserve capacity of 10% and 20%

tail" when the reserve capacity increases to more than 20%. These results do suggest to us that increasing the capacity of system spinning reserve would substantially reduce the risk of large blackouts.

Recall from last subsection that we found a critical point at which the loading level is close to available generation. Usually the generation and load are set such that the line flows are well below line limits. Therefore, the power tail can possibly be "fixed" (i.e. changed to exponential tail) by supplying ample spinning reserve. It seems that the role of reserve is to eliminate the critical point. While it is not the case considering the load growth. Suppose that the load keeps growing without line upgrading (i.e., line limits remain the same), then finally the load level will approach the full system capacity, meanwhile the available reserve capacity will keep dropping even to zero due to line limits. Associated with this scenario, the "fixed" exponential tail will be changed back to the power tail, thus a shifted critical point appears. Therefore, the reserve can put off the critical region but can not eliminate it because of line limits.

3.3. Impact of Hidden Failure Probability

Hidden failure probability, p, is another important parameter in this model. Its impact on the system behavior is of great interest to us. Figure **??** shows the probability distribution of blackout size with different hidden failure probabilities. As we can see, the power tail preserves but becomes steeper as p decreases, which means reducing the hidden failure in the protection system makes the system more robust. For example, upgrading old protection system or perhaps consistent maintenance will shift the observed power tail downwards. But, unfortunately, the system does not go through dramatic change by varying hidden failure probabilities (i.e. the power tail remains).

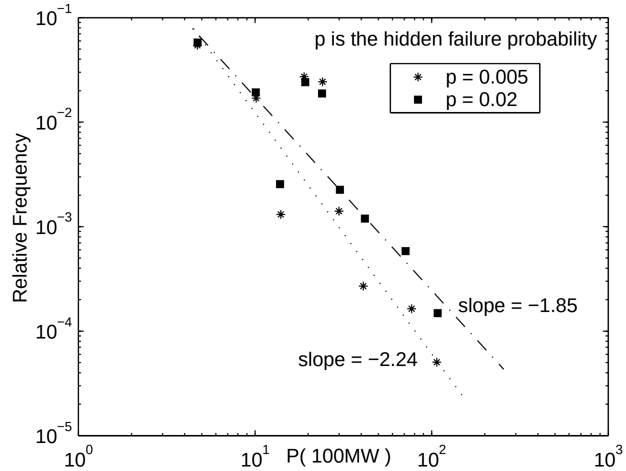

Figure 7. Distribution of blackout size P with different hidden failure probabilities

Thorp et al. have also explored the hidden failures in protective relays and their impact on power transmission system reliability in recent studies [4,6]. The previous work focused on detection of the weakest links in the bulk power system and correspondent economical system upgrading strategy under "limited budget" assuming only several weak links can be improved. While our focus here is to investigate similar problem but with "unlimited budget", in which case we assume all lines can be improved at the same rate. Although this is far away from optimum, it does give an sort of "upper bound" for achievable improvement of system reliability. For example, suppose the p of current protection system is 0.02, and we can reduce p at most to 0.005. Then any optimal system upgrading strategy with limited budget, such as aforementioned studies, will generate a new pdf located somewhere between the two power tails shown in Figure **??**. The power tail with $p = 0.005$ is therefore the "upper bound". It would be nice to develop a system upgrading scheme that can closely approach this bound, but it is beyond the scope of this paper.

A "by product" obtained from this analysis is the rough order of magnitude of p. The idea is to adjust p to generate the same power tail from NERC data. Recall from [1,3] that the power exponent is around -2, we found out the rough order of p is 10^{-2}. Another way to estimate p is by the following calculation.

Since the major disturbances typically involve four to five unlikely hidden failures, the approximate probability of one typical sample path will be p^{-5}. According to NERC report [3], around 200 events happened in WSCC area during the past 16 years. Assume one cascading event could be initiated in every power circle, thus the probability of one event will be approximately $150/(16 \times 365 \times 24 \times 60 \times 60 \times 60) = 5.4 \times 10^{-9} = p^{-5}$. Again, $p \simeq 10^{-2}$.

3.4. Impact of Control Strategy

Typical major blackouts involve not only hidden failure trips but also overloading line outages. Improved robust protection system will reduce the risk incurred by hidden failures, while various prompt system control will play the role of preventing cascading overloads.

The only control used in the model is LP redispatch, which is highly equivalent various control strategies in real systems. The only adjustable parameter here is the responding speed of LP redispatch to cascading overloads. To simplify the implementation, regular LP redispatch is used, say, one redispatch every three trips. Notice that LP redispatch is effective only when there exist overloads in the system, but won't change the system state if no line constraint violation. Besides the regular checkpionts, redispatch will be performed additionally whenever the system breaks into islands.

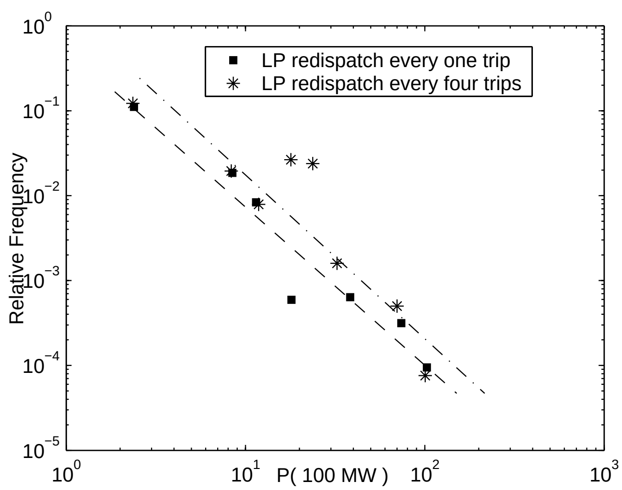

Figure 8. Distribution of blackout size P with different LP redispatchs

When a cascading event is triggered, the sooner the system back to "normal" with no overloads, the better. The pdf of blackout size in Figure **??** shows that the power tail is shifted downwards when the "regular" interval is changed from once every four trips to once every trip. And the measured expected power loss reduces almost 60%. Here, once every trip means every overload is "captured", while once every four trips indicates possible cascading overloads. The gap between does indicate the improvement we can achieve by adding prompt control. If we can not take any precaution against possible cascading outages, "once per trip" is the best we can do to prevent disturbances further spreading. The power tail then is the " upper bound" when evaluating the system reliability with respect to system control.

4. Conclusion

A DC model with an improved hidden failure mechanism has been developed to investigate the cascading behavior of power transmission systems. We examined the impacts of various parameters on system dynamics. In particular,

(1) The system shows power law behavior near a critical loading, at which the expected power loss increases sharply.

(2) Maintaining ample spinning reserve can greatly reduce the risk of big blackouts. The system shows exponential tails with high reserve capacity but power tails as reserve capacity goes down.

(3) More robust protection system (with reduced hidden failure probabilities) will increase the system reliability. The system still exhibits power law behavior but with steeper slopes.

(4) Prompt control actions will prevent cascading overloads hence further reducing the risk of big disturbances. The power tail is shifted down with faster control actions.

The tradeoff among these parameters with respect to system reliability and economic operation is essential to power system design or reconstruction. Although it turns out to be complicated and beyond the scope of this paper, the fully understanding of it would have significant consequences for power system operation and hence is worth further investigating.

References

[1] J.Chen, J.S.Thorp, M.Parashar, Analysis of Electric Power Disturbance Data, 34th Hawaii International Conference on System Sciences, Maui, Hawaii, January 2001

[2] I.Dobson, J. Chen, J.S. Thorp, B.A.Carreras, D.E.Newman, Examining criticality of blackouts in power system models with cascading events, 35th Hawaii International Conference on System Sciences, Hawaii, January 2001

[3] Information on electric systems disturbances in North America can be downloaded from the NERC website at http://www.nerc.com/dawg/database.html

[4] K.Bae, J.S.Thorp, A Stochastic Study of Hidden Failures in Power System Protection, Decision Support Systems 24, pp259-268, 1999

[5] J.S.Thorp, A.G. Phadke, et al., Anatomy of Power System Disturbances: Importance Sampling, PSCC, Dresden, Aug. 1996

[6] H.Wang, J.S.Thorp, Enhancing Reliability of Power Protection Systems Economically in the Post-Restructuring Era, NAPS, 2000

[7] J.A. Bucklew, Large Deviation Techniques in Decision, Simulation, and Estimation. John Wiley and Sons, Inc. 1990

6.4 Evidence for self-organized criticality in a time series of electric power system blackouts

B.A. Carreras, D.E. Newman, I. Dobson, A.B. Poole

preprint; submitted to IEEE Transactions on Power Systems

Evidence for Self-Organized Criticality in a Time Series of Electric Power System Blackouts

Benjamin A. Carreras, David E. Newman, Ian Dobson, and A. Bruce Poole

Abstract— **We analyze a 15-year time series of North American electric power transmission system blackouts for evidence of self-organized criticality. The probability distribution functions of various measures of blackout size have a power tail and R/S analysis of the time series shows moderate long time correlations. Moreover, the same analysis applied to a time series from a sandpile model known to be self-organized critical gives results of the same form. Thus the blackout data is consistent with self-organized criticality. A qualitative explanation of complex dynamics observed in electric power system blackouts is suggested.**

Keywords— **blackouts, complex systems, time series, power system security, reliability, risk analysis.**

I. Introduction

Electric power transmission networks are complex systems that are commonly run near their operational limits. Major cascading disturbances, or blackouts of these transmission systems have serious consequences. Individually, these blackouts can be attributed to specific causes, such as lightning strikes, ice storms, equipment failure, shorts resulting from untrimmed trees, excessive customer load demand, or unusual operating conditions. However, an exclusive focus on these individual causes can overlook the global dynamics of a complex system in which repeated major disruptions from a wide variety of sources are a virtual certainty. We analyze a time series of blackouts to probe the nature of these complex system dynamics.

The North American Electrical Reliability Council (NERC) has a documented list summarizing major blackouts of the North American power grid [1]. They are of diverse magnitude and of varying causes. It is not clear how complete this data is, but it is the best-documented source that we have found for blackouts in the North American power transmission system. An initial analysis of these data [7] over a period of 5 years suggested that self-organized criticality (SOC) [2], [3], [16] may govern the complex dynamics of these blackouts. Here we further examine [8], [11] this hypothesis by extending the analysis to 15 years. This extended data allows us to develop improved statistics and gives us longer time scales to explore. We compare the results to the same types of analysis of time sequences generated by a sandpile model known to be SOC. The similarity of the results is quite striking and is suggestive of the possible role that SOC plays in power system blackouts. A plausible qualitative explanation of SOC in power system blackouts is outlined in section VI.

As an introduction to the concept, a SOC system is one in which the nonlinear dynamics in the presence of perturbations organize the overall average system state near to, but not at, the state that is marginal to major disruptions. SOC systems are characterized by a spectrum of spatial and temporal scales of the disruptions that exist in remarkably similar forms in a wide variety of physical systems [2], [3], [16]. In these systems, the probability of occurrence of large disruptive events decreases as a power function of the event size. This is in contrast to Gaussian systems in which this probability decays exponentially with event size. One important implication of this type of dynamics is in calculating the risk of large blackouts. Because of the power law tail in the probability distribution function of the events, standard risk probability techniques would no longer be valid when analyzing the low probability tails. This would require reanalysis of the risks in light of these dynamics.

II. Time series of blackout data

We have analyzed the full 15 years of data from 1984 to 1998 that is publicly available from NERC [1]. There are 427 blackouts in 15 years and 28.5 blackouts per year. The average period of time between blackouts is 12 days. The blackouts are distributed over the 15 years in an irregular manner. We have detected no evidence of systematic changes in the number of blackouts or periodic or quasi-periodic behavior. However, it is difficult to determine long term trends or periodic behavior in just 15 years of data. We constructed time series from the NERC data with the resolution of a day for the number of blackouts and for three different measures of the blackout size. The length of the time record is 5477 days. The three measures of blackout size are:

1. energy unserved (MWh)
2. amount of power lost (MW)
3. number of customers affected.

Energy unserved was estimated from the NERC data by multiplying the power lost by the restoration time.

Submitted December 2001. B. A. Carreras is with Oak Ridge National Laboratory, Oak Ridge TN 37831 USA; email: carreras@fed.ornl.gov. D.E. Newman is with the Physics department, University of Alaska, Fairbanks AK 99775 USA; email ffden@uaf.edu. Ian Dobson is with the ECE department, University of Wisconsin, Madison WI 53706 USA; email dobson@engr.wisc.edu. A.B. Poole is with the Federal Energy Regulatory Commission in Washington DC; email bruce.poole@ferc.fed.us. Part of this research has been carried out at Oak Ridge National Laboratory, managed by UT-Battelle, LLC, for the U.S. Department of Energy under contract number DE-AC05-00OR22725. Part of this research was coordinated by the Consortium for Electric Reliability Technology Solutions and was funded by the Assistant Secretary for Energy Efficiency and Renewable Energy, Office of Power Technologies, Transmission Reliability Program of the U.S. Department of Energy under contract number DE-AC05-00OR22725 and DE-A1099EE35075 with the National Science Foundation. I. Dobson and D.E. Newman gratefully acknowledge support in part from National Science Foundation grants ECS-0085711 and ECS-0085647.

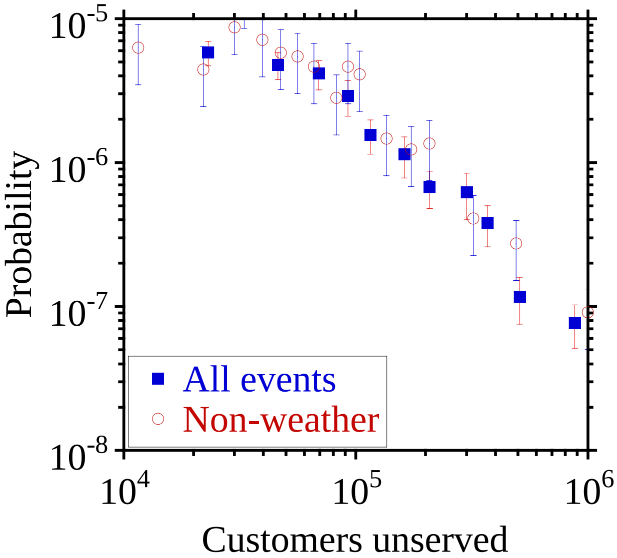

Fig. 1. PDF of the number of customers unserved comparing the total data set with the data excluding the weather related events.

III. Analysis of the blackout time series

In order to gain an understanding of the dynamics of a system from analysis of a time series, one must employ a variety of tools beyond basic statistical analysis. Among other measures which should be employed, the tails of the Probability Distribution Function (PDF) should be investigated for normality and frequency spectra should be viewed in order to begin to look at dependencies in the time domain. The time domain is particularly important as the system dynamics are expressed in time. Periodicities and long time correlations must both be examined and compared to systems with known dynamics. We will present details of the analysis of the PDFs later; however, the first striking characteristic of the data is the power law tail of these PDFs. This power law tail is shown in Fig. 1, where we have plotted the PDF of the number of customers unserved for all events (the squares) on a log-log plot. The PDF falls off with a power of approximately –1.7 which implies a divergent variance and a clearly non-normal distribution.

Looking in the time domain, a time series is said to have long range dependence if its autocorrelation function falls off asymptotically as a power law. This type of dependence is difficult to determine because noise tends to dominate the signal for long time lags. One way to address this problem is the rescaled range statistics (R/S statistics) proposed by Mandelbrot and Wallis [17] and based on a previous hydrological analysis by Hurst [14]. The R/S statistics considers blocks of m successive points in the integrated time series and measures how fast the range of the blocks grows as m increases. The calculation of the R/S statistics is further described in the Appendix.

It can be shown that in the case of a time series X with an autocorrelation function that has an algebraic tail, the R/S statistic scales proportionally to m^H, where H is the Hurst exponent. Thus H is the asymptotic slope on a log-log plot of the R/S statistic versus the time lag. If $1 > H > 0.5$, there are long range time correlations, for $0.5 > H > 0$, the series has long range anticorrelations, and if $H = 1.0$, the process is deterministic. Uncorrelated noise corresponds to $H = 0.5$. A constant H parameter over a long range of time lag values is consistent with self-similarity of the signal in this range [21] and with an autocorrelation function that decays as a power of the time lag with exponent $2 - 2H$.

We have determined the long range correlations in the 15 year blackout time series using the R/S method. The time series has 5477 days and 427 blackouts. The calculated Hurst exponents [14] for the different measures of blackout size are shown in Table I. The H values are obtained by fitting over time lags between 100 and 3000 days. In this range, the behavior of the R/S statistic is power-like (Fig. 5). The values of H obtained for all the time series are close to 0.6. This seems to indicate that they are all equally correlated over the long range. These values of H are somewhat lower than the previously obtained values [7], but still significantly above 0.5. Note that the “events” in the time series are the events that have produced a blackout and not all the events that occurred. The latter are supposed to be random ($H = 0.5$); however, the events that produce a blackout may indeed have moderate correlations because they depend on the state of the system.

TABLE I

Hurst parameter H from R/S analysis of blackout size time series

	H
Events	0.62
Power lost	0.59
Customers	0.57
MWh	0.53

A method of testing the independence of the triggering events has been suggested by Boffetta et al. [4]. They evaluated the times between events (waiting times) and argued that the PDF of the waiting times should have an exponential tail. Such is clearly the case for the waiting times of sandpile avalanches (Fig. 2). In the case of waiting times between blackouts, we also have observed the same exponential dependence of the PDF tail (Fig. 3). This observation is confirmed in [11]. This strengthens the contention that the apparent correlations in the events come from SOC-like dynamics within the power system rather than from the events driving the power system dynamics.

Examining the R/S results in more detail, Fig. 4 shows the R/S statistic for the time series of the number of customers affected by blackouts. The average period of time without blackouts is 12 days, hence, in looking over time lags of this order we typically find either one blackout or none. For the shorter time lags less than 50 days, we are unable to get information on correlations between black-

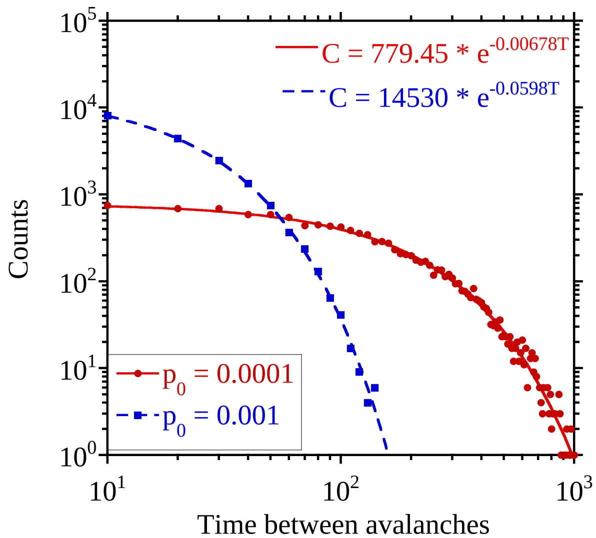

Fig. 2. Distribution of waiting times between avalanches in a sandpile for two values of the probability of adding grains of sand.

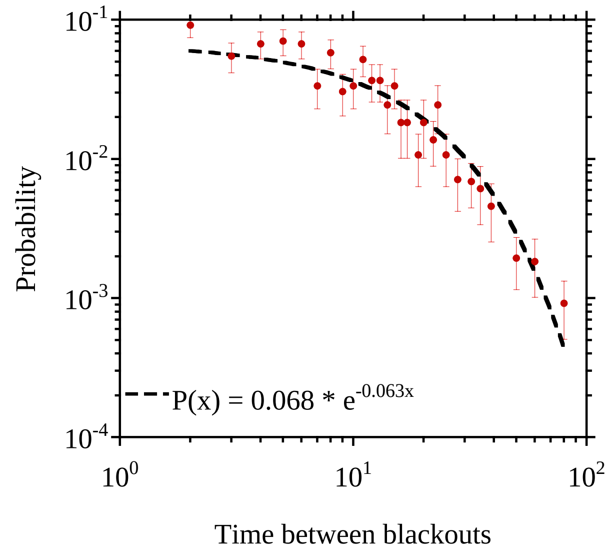

Fig. 3. PDF of the waiting times between blackouts

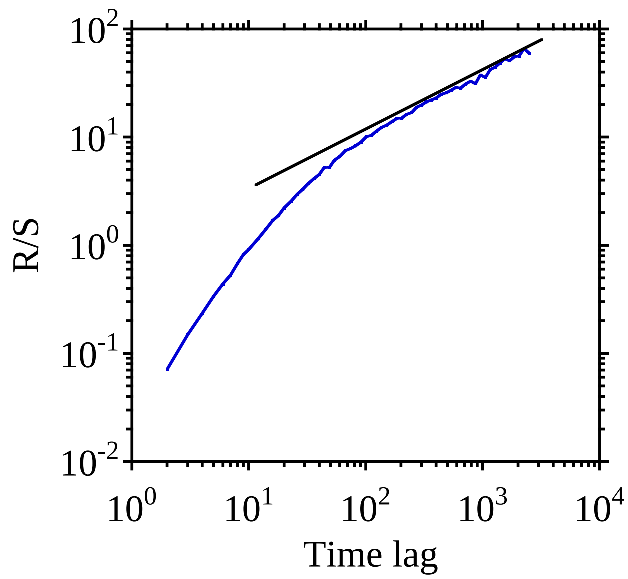

Fig. 4. R/S for the number of customers affected by blackouts.

outs because the time intervals are too short to contain several blackouts. We see a correlation between absences of blackouts, and because these time intervals tend to only contain absences of blackouts, we see H close to 1 (trivially deterministic). For time lags above 50 days, the R/S shows a power behavior and gives a correct determination of blackout correlation. The R/S calculation is sensitive to this change in regime and there is an obvious change of behavior for time intervals around 50 days. An alternative method of determining correlations is the scaled window variance (SWV) method. We do not use the scaled window variance method in this paper because in this method, the correlations between absences of blackouts skew the correlations between blackouts at larger time lags [8].

IV. The effect of weather

Approximately half of the blackouts (212 blackouts) are characterized as weather related in the NERC data. In attempting to extract a possible periodicity related to seasonal weather, we consider separately the time series of all blackouts and the time series of blackouts that are not weather related. An important issue in studying long range dependencies is the possible presence of periodicities. Both R/S analysis and spectral analysis of this data do not show any clear periodicity. However, since the weather related events may play an important role in the blackouts, one may suspect seasonal periodicities. However, the data combines both summer and winter peaking regions of North America. Because of the limited amount of data, it is not possible to separate the blackouts by geographical location and redo the analysis. What we have done is to reanalyze the data excluding the blackouts triggered by weather related events. The results are summarized in Table II. As can be seen, the exclusion of the blackouts triggered by weather related events does not significantly change the value of H. When looking solely at the blackouts triggered by weather related events, the value of H is closer to 0.5 (random events), although the available data is too sparse to be sure of the significance of this result.

Another question to consider is the effect of excluding the weather related events on the PDF. We have recalculated the PDF for all the measures of blackout size when the weather related events are not included. The PDFs obtained are the same within the numerical accuracy of this calculation. This is illustrated in Fig. 1, where we have

TABLE II
Hurst parameter H for measures of blackout size comparing all data with the data excluding blackouts triggered by weather.

	H all events	H non weather events
Events	0.62	0.62
Power lost	0.59	0.64
Customers	0.57	0.58
MWh	0.53	0.57

plotted the PDFs of the number of customers unserved for all events and for the non-weather related events. Therefore, for both long range dependencies and structure of the PDF, the blackouts triggered by weather events do not show any particular properties that distinguish them from the other blackouts. Therefore, both the long time correlations and the PDFs of the blackout sizes remain consistent with SOC-like dynamics.

In addition to weather effects, one might expect spatial structure of the grid to have an effect on the dynamics. However, analysis of the NERC data in [11] suggests that similar results are obtained when data for the eastern and western North American power systems is analyzed separately. Since the eastern and western power systems have different characteristics, this interesting result tends to support the notion that there are some underlying common principles for the system dynamics.

V. Comparison to a SOC sandpile model

The issue of determining whether the power system blackouts are governed by SOC is a difficult one. There are no unequivocal determining criteria. One approach is to compare characteristic measures of the power system to those obtained from a known SOC system. The prototypical model of a SOC system is a one-dimensional idealized running sandpile [15]. The mass of the sandpile is increased by adding grains of sand at random locations. However, if the height at a given location exceeds a threshold, then grains of sand topple downhill. The topplings cascade in avalanches that transport sand to the edge of the sandpile, where the sand is removed. In the running sandpile, the addition of sand is on average balanced by the loss of sand at the edges and there is a globally quasi-steady state or dynamic equilibrium close to the critical profile that is given by the angle of repose. There are avalanches of all sizes and the PDF of the avalanche sizes has an algebraic tail. The particular form of the sandpile model used here is explained in [18] and the sandpile length used in the present calculations is $L = 800$. We are, of course, not claiming that the running sandpile is a model for power system blackouts. We only use the running sandpile as a black box to produce a time series of avalanches characteristic of an SOC system.

It is convenient to assume that every time iteration of the sandpile corresponds to one day. When an avalanche

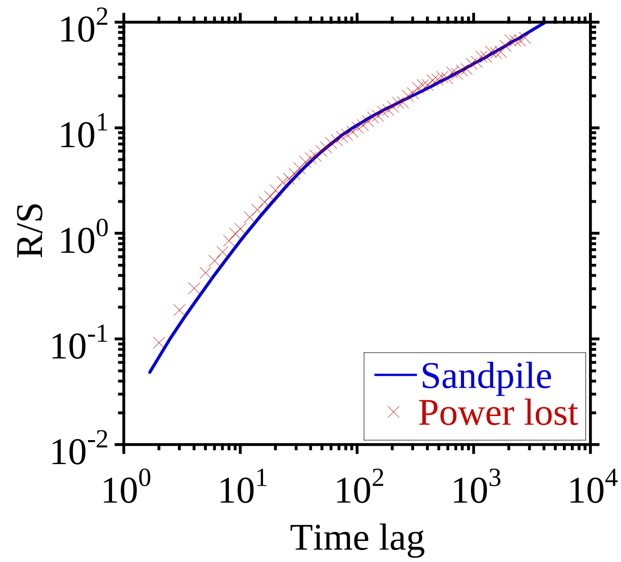

Fig. 5. R/S for avalanche sizes in a running sandpile compared to R/S for power lost in blackouts.

starts, we integrate over the number of sites affected and the number of steps taken and assign them to a single day. Thus we construct a time series of the avalanche sizes. The sandpile model has a free parameter p_0, which is the probability of a grain of sand being added at a location. p_0 is chosen so that the average frequency of avalanches is the same as the average frequency of blackouts.

In evaluating the long range time dependence of the blackouts, we use the rescaled range or R/S [17] technique described earlier. As stated before, the R/S technique is useful in determining the existence of an algebraic tail in the autocorrelation function and calculating the exponent of the decay of the tail (see Appendix for details). The same R/S analysis used for the blackout time series is applied to the avalanche time series. Fig. 5 shows the R/S statistic for the time series of avalanche sizes from the sandpile and for the time series of power lost by the blackouts. The similarity between the two curves is remarkable. A similarly good match of the R/S statistics between the blackout and sandpile time series is obtained for the other measures of blackout size.

Fig. 6 shows the PDF of the avalanche sizes from the sandpile data together with the rescaled PDF of the energy unserved from the blackout data. The resemblance between the two functions is again remarkable. The rescaling is necessary because of the different units used to measure avalanche size and blackout size. That is, we assume a transformation of the form

$$P(X) = \lambda F(X/\lambda) \tag{1}$$

X is the variable that we are considering, $P(X)$ is the corresponding PDF, and λ is the rescaling parameter. If the transformation (1) works, F is the universal function that

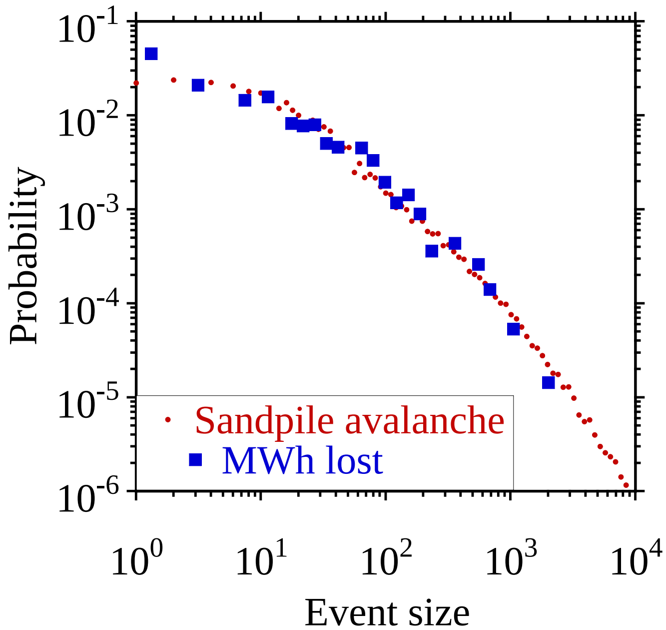

Fig. 6. Rescaled PDF of energy unserved during blackouts superimposed on the PDF of the avalanche size in the running sandpile.

describes the PDF for the different parameters. Transformation (1) is used to overlay the sandpile and blackout PDFs.

We can consider PDFs of the other measures of blackout size and use transformation (1) to plot each of these PDFs with the sandpile avalanche size PDF. In all cases, the agreement is very good. Of course, the scaling parameter differs for each measure of blackout size. The exponents obtained for these PDFs tails are between -1.3 and -2. These exponents imply divergence of the variance, one of the characteristic features of systems with SOC dynamics. In fact, divergence of the variance is a general feature of systems near criticality. This comparison of the PDFs of the measures of blackout and avalanche sizes is useful in evaluating the possible errors in the determination of the algebraic decay exponent of the PDFs. One can see that for the large size events where the statistics are sparse, there may be deviations from the curve. These deviations can influence the computed value of the exponent, but they are probably of little significance for the present comparisons.

VI. Possible explanation of power system self-organized criticality

To motivate comparisons between power system blackout data and SOC sandpile data, we suggest a qualitative description of the structure and effects in a large scale electric power transmission system which could give rise to SOC dynamics. The power system contains many components such as generators, transmission lines, transformers and substations. Each component experiences a certain loading each day and when all the components are considered together they experience some pattern or vector of loadings. The pattern of component loadings is determined by the power system operating policy and is driven by the aggregated customer loads at substations. The power system operating policy includes short term actions such as generator dispatch as well as longer term actions such as improvements in procedures and planned outages for maintenance. The operating policy seeks to satisfy the customer loads at least cost. The aggregated customer load has daily and seasonal cycles and a slow secular increase of about 2% per year.

Events are either the limiting of a component loading to a maximum or the zeroing of the component loading if that component trips or fails. Events occur with a probability that depends on the component loading. For example, the probability of relay misoperation [11] or transformer failure generally increases with loading. Another example of an event could be an operator redispatching to limit power flow on a transmission line to its thermal rating and this could be modeled as probability zero when below the thermal rating of the line and probability one when above the thermal rating. Each event is a limiting or zeroing of load in a component and causes a redistribution of power flow in the network and hence a discrete increase in the loading of other system components. Thus events can cascade. If a cascade of events includes limiting or zeroing the load at substations, it is a blackout. A stressed power system experiencing an event must either redistribute load satisfactorily or shed some load at substations in a blackout. A cascade of events leading to blackout usually occurs on a time scale of minutes to hours and is completed in less than one day.

It is customary for utility engineers to make prodigious efforts to avoid blackouts and especially to avoid repeated blackouts with similar causes. These engineering responses to a blackout occur on a range of time scales longer than one day. Responses include repair of damaged equipment, more frequent maintenance, changes in operating policy away from the specific conditions causing the blackout, installing new equipment to increase system capacity, and adjusting or adding system alarms or controls. The responses reduce the probability of events in components related to the blackout, either by lowering their probabilities directly or by reducing component loading by increasing component capacity or by transferring some of the loading to other components. The responses are directed towards the components involved in causing the blackout. Thus the probability of a similar blackout occurring is reduced, at least until load growth degrades the improvements made. There are similar, but less intense responses to unrealized threats to system security such as near misses and simulated blackouts.

The pattern or vector of component loadings may be thought of as a system state. Maximum component loadings are driven up by the slow increase in customer loads via the operating policy. High loadings increase the chances of cascading events and blackouts. The loadings of components involved in the blackout are reduced or relaxed by the engineering responses to security threats and blackouts. However, the loadings of some components not involved in the blackout may increase. These opposing forces driving the component loadings up and relaxing the component loadings are a reflection of the standard tradeoff between satisfying customer loads economically and security. The opposing forces apply over a range of time scales. We suggest that the opposing forces, together with the underlying growth in customer load and diversity give rise to a dynamic equilibrium and conjecture that this dynamic equilibrium could be SOC. It is important to note that this type of system organizes itself to an operating point near to but not at a critical value. This could make the system intrinsically vulnerable to cascading failures from unexpected causes as the repair and remediation steps taken to prevent a known failure mode are part of the system dynamics.

We briefly indicate the roughly analogous structure and effects in an idealized sand pile model. Events are the toppling of sand and cascading events are avalanches. The system state is a vector of maximum gradients at all the locations in the sand pile. The driving force is the addition of sand, which tends to increase the maximum gradient, and the relaxing force is gravity, which topples the sand and reduces the maximum gradient. SOC is a dynamic equilibrium in which avalanches of all sizes occur and in which there are long time correlations between avalanches. The rough analogy between the sand pile and the power system is shown in Table III. There are also some distinctions between the two systems. In the sand pile, the avalanches are coincident with the relaxation of high gradients. In the power system, each blackout occurs on fast time scale (less than one day), but the knowledge of which components caused the blackout determines which component loadings are relaxed both immediately after the blackout and for some time after the blackout.

TABLE III

Analogy between power system and sand pile.

	power system	sand pile
system state	loading pattern	gradient profile
driving force	customer load	addition of sand
relaxing force	response to blackout	gravity
event	limit flow or trip	sand topples

VII. Conclusions

We have calculated long time correlations and PDFs for several measurements of blackout size in the North American power transmission grid from 1984 to 1998. These long time correlations and PDFs are consistent with long range time dependencies and PDFs for avalanche sizes in a running sandpile known to be SOC. That is, for these statistics, the blackout size time series is indistinguishable from the sandpile avalanche size time series. This similarity suggests that SOC dynamics may play an important role in the global complex dynamics of power systems.

We have outlined a possible qualitative explanation of the complex dynamics in a power system which proposes some of the opposing forces that could give rise to a dynamic equilibrium with SOC properties. The opposing forces are, roughly speaking, a slow increase in loading (and system aging) weakening the system and the engineering responses to blackouts strengthening parts of the system. Here we are suggesting that the engineering and operating policies of the system are important and integral parts of the system dynamics.

The probability distribution functions of the measures of blackout size have power tails with exponents ranging from -1.3 to -2 and therefore have divergent variances. Thus large blackouts are much more frequent than might be expected. In particular, the application of traditional risk evaluation methods can underestimate the risk of large blackouts. R/S analysis of the blackout time series shows moderate ($H \approx 0.6$) long time correlations for several measures of blackout size. Excluding the weather related blackouts from the time series has little effect on the results. The exponential tail of the PDF of the times between blackouts supports the contention that the correlations between blackouts are due to the power system global dynamics rather than correlations in the events that trigger blackouts.

The strength of our conclusions is naturally somewhat limited by the short time period (15 years) of the available blackout data and the consequent limited resolution of the statistics. To further understand the mechanisms governing the complex dynamics of power system blackouts, modeling of the power system from a SOC perspective and other perspectives is indicated and is underway [12], [9], [20], [11], [10], [13], [19], [6].

If the dynamics of blackouts are confirmed to be SOC, this would open possibilities for monitoring statistical precursors of large blackouts or even controlling the power system to modify the expected distribution of blackout sizes. Most importantly, it would suggest the need to revisit the traditional risk analysis based on normal statistics since these complex systems have very non-normal statistics.

VIII. Acknowledgements

We thank J.S. Thorp for useful discussions. Ian Dobson thanks H-D. Chiang and the School of Electrical Engineering at Cornell University for their generous hospitality during a sabbatical leave.

References

[1] Information on blackouts in North America can be downloaded from the NERC website at http://www.nerc.com/dawg/database.html.

[2] P. Bak, C. Tang, and K. Wiesenfeld, Self-organized criticality: an explanation of 1/f noise, Phys. Rev. Lett., vol. 59, pp. 381-4, 1987.

[3] P. Bak, How nature works: the science of self-organized criticality, Copernicus books, 1996.

[4] G. Boffetta, V. Carbone, P. Guliani, P. Veltri, A. Vulpiani, Power laws in solar flares: self-organized criticality or turbulence? Phys. Rev. Letters, vol. 83, pp. 4662-4665, 1999.

[5] M. J. Cannon, D. B. Percival, D. C. Caccia, G. M. Raymond, J. B. Bassingthwaighte, Evaluating scaled windowed variance methods for estimating the Hurst coefficient of time series, Physica A, vol. 241, pp. 606-626, 1997.

[6] J.M. Carlson, J. Doyle, Highly optimized tolerance: a mechanism for power laws in designed systems, Physical Review E, vol. 60, 1999, pp. 1412-1427.

[7] B. A. Carreras, D. E. Newman, I. Dobson, and A. B. Poole, Initial evidence for self-organized criticality in electric power blackouts, 33rd Hawaii International Conference on System Sciences, Maui, Hawaii, Jan. 2000.
[8] B.A. Carreras, D.E. Newman, I. Dobson, A.B. Poole, Evidence for self organized criticality in electric power system blackouts, Thirty-fourth Hawaii International Conference on System Sciences, Maui, Hawaii, January 2001
[9] B.A. Carreras, V.E. Lynch, M. L. Sachtjen, I. Dobson, D. E. Newman, Modeling blackout dynamics in power transmission networks with simple structure, 34th Hawaii International Conference on System Sciences, Maui, Hawaii, January 2001.
[10] B.A. Carreras, V.E. Lynch, I. Dobson, D.E. Newman, Dynamics, criticality and self-organization in a model for blackouts in power transmission systems, Thirty-fifth Hawaii International Conference on System Sciences, Hawaii, January 2002.
[11] J. Chen, J.S. Thorp, M. Parashar, Analysis of electric power system disturbance data, Thirty-fourth Hawaii International Conference on System Sciences, Maui, Hawaii, January 2001.
[12] I. Dobson, B. A. Carreras, V.E. Lynch, D. E. Newman, An initial model for complex dynamics in electric power system blackouts, 34th Hawaii International Conference on System Sciences, Maui, Hawaii, Jan. 2001.
[13] I. Dobson, J. Chen, J.S. Thorp, B.A. Carreras, D.E. Newman, Examining criticality of blackouts in power system models with cascading events, Thirty-fifth Hawaii International Conference on System Sciences, Hawaii, January 2002.
[14] H. E. Hurst, Long-term storage capacity of reservoirs, Trans. Am. Soc. Civil Eng., vol. 116, pp. 770, 1951.
[15] T. Hwa and M. Kardar, Avalanches, hydrodynamics, and discharge events in models of sandpiles, Physical Review A, vol. 45, no. 10 pp. 7002-7023, May 1992.
[16] H.J. Jensen, Self-organized criticality, Cambridge University Press, 1998.
[17] B. B. Mandelbrot and J. R. Wallis, Noah, Joseph, and operational hydrology, Water Resources Research, vol. 4, pp. 909-918, 1969.
[18] D. E. Newman, B. A. Carreras, P. H. Diamond, T.S. Hahm, The dynamics of marginality and self-organized criticality as a paradigm turbulent transport, Physics of Plasmas, vol. 3, no. 5, pp. 1858-1866, Part 2, May 1996.
[19] S. Roy, C. Asavathiratham, B. C. Lesieutre, G. C. Verghese, Network models: growth, dynamics, and failure, 34th Hawaii International Conference on System Sciences, Maui, Hawaii, Jan. 2001.
[20] M. L. Sachtjen, B. A. Carreras, and V. E. Lynch, Disturbances in a power transmission system, Physical Review E, vol. 61, no. 5, May 2000, pp. 4877-4882.
[21] G. Samorodnitsky and M. S. Taqqu, Stable Non-Gaussian Random Processes: Stochastic Models with Infinite Variance, New York: Chapman and Hall, 1994.

Appendix

Consider the time series $X = \{X_t; t = 1, 2, ..., n\}$. We construct the series $Y = \{Y_t; t = 1, 2, ..., n\}$ that is the original series integrated in time: $Y_t = \sum_{s=0}^{t} X_s$. For the series Y and for each $m = 1, 2, ..., n$ a new series $Y^{(m)} = \{Y_u^{(m)}; u = 1, 2, ..., n/m\}$ is generated. The elements of the series $Y^{(m)}$ are blocks of m elements of Y so that $Y_u^{(m)} = \{Y_{um-m+1}^{(m)}, ..., Y_{um}\}$. We then calculate the range R_m^i and standard deviation S_m^i within each of the n/m blocks of m elements of $Y^{(m)}$, and compute for each block R_m^i/S_m^i. The R/S statistic as a function of the time lag m is then the average $\frac{m}{n}\sum_{i=1}^{n/m} R_m^i/S_m^i$.

Benjamin A. Carreras received the Licenciado en Ciencias degree in Physics from the University of Barcelona, Spain in 1965 and the PhD degree in Physics from Valencia University, Spain in 1968. He has worked as a researcher or as a professor at the University of Madrid, Spain, Glasgow University, Scotland, Daresbury Nuclear Physics Laboratory, England, Junta de Energia Nuclear, Madrid, Spain, and the Institute for Advanced Study, Princeton, NJ USA. He is now corporate fellow at Oak Ridge National Lab, TN USA. He is a fellow of the American Physical Society.

David E. Newman received the BS degree in Physics and Mathematics from the University of Pittsburgh, PA in 1983 and the Ph.D. degree in Physics from the University of Wisconsin, Madison, WI in 1993. He was a Wigner fellow and research scientist at Oak Ridge National Laboratory from 1993 to 1998. In 1998 he joined the Physics department at the University of Alaska, Fairbanks, where he is now associate professor.

Ian Dobson received the BA degree in Mathematics from Cambridge, England in 1978 and the PhD degree in Electrical Engineering from Cornell University in 1989. He worked from 1978 to 1983 as a systems analyst for the British firm EASAMS Ltd. In 1989 he joined the University of Wisconsin-Madison, where he is now a professor in electrical and computer engineering. His current interests are applications of nonlinear dynamics, electric power system instabilities, power electronics and complex systems.

A. Bruce Poole received the B.S. degree in Aerospace/ Mechanical Engineering from the University of Texas in 1968 and the M. A. in Management from Tusculum College in 1992. He worked as engineer and manager for a variety of manufacturing and utility companies, including Westinghouse Electric Corporation, Houston Lighting and Power Company, and the Tennessee Valley Authority. He worked at Oak Ridge National Lab, TN USA from 1989 to 2000, where he was a senior research staff member and program manager. He presently works for the Federal Energy Regulatory Commission in Washington DC.